

**AN EXPERIMENTAL INVESTIGATIONS INTO THE
PERFORMANCE OF NANOREFRIGERANTS (R134a+Al₂O₃,
R134a+SiO₂) BASED REFRIGERATION SYSTEM**

*Thesis submitted in partial fulfillment of requirement for the award of the
degree of*

Master of Engineering

IN

THERMAL ENGINEERING

Submitted By:

SATNAM SINGH

Roll No. 801283026

Under the supervision of

Mr. Kundan Lal, Assistant Professor

Department of Mechanical Engineering,

Thapar University, Patiala




DEPARTMENT OF MECHANICAL ENGINEERING

THAPAR UNIVERSITY, PATIALA-147004, INDIA, JULY 2014

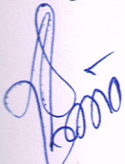
**Established under section 3 of UGC Act, 1956 vide notification # F-12/84-U.3 of
Government of India.**

DECLARATION

I hereby declare that thesis entitled "An Experimental Investigations into the Performance of Nanorefrigerants (R134a+Al₂O₃, R134+SiO₂) Based Refrigeration System " is an authentic record of my study carried out as requirements for award of the degree of M.E (Thermal Engineering) at Thapar University, Patiala, under the supervision of Mr. Kundan Lal, Assistant Professor, Department of Mechanical Engineering, Thapar University, Patiala during August 2013 to July 2014 .The matter presented in this thesis has not been submitted for the award of any other degree of this or any other university.


(SATNAM SINGH)

This is to certify that the above declaration made by the student concerned is correct to best of my knowledge and belief.

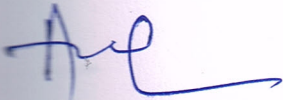


(Mr. KUNDAN LAL)

Assistant Professor,

Thapar University, Patiala-147004

Countersigned by



(Dr. AJAY BATISH)

Professor & Head

Department of Mechanical Engineering

Thapar University, Patiala-147004


(Dr. S.K. MOHAPATRA)

Dean of Academic Affairs

Thapar University, Patiala-147004

ACKNOWLEDGEMENT

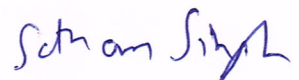
At first, thanks to the almighty for his abundant blessing showered on me throughout this Endeavour to complete this work successfully.

My honorable guide Mr. Kundan Lal, Assistant Professor, Department of Mechanical Engineering, is a person to whom I shall always remain grateful for his excellent guidance, valuable discussions, encouragement, constructive criticism and his insights have strengthened this study significantly. He gave me a complete freedom to use my opinion, correcting whenever necessary in my dissertation.

I would like to thanks to Dr. Ajay Batish, Head of the Mechanical Engineering Department, and Dr. S.K Mohapatra Dean of Academic Affairs, Thapar University Patiala, who has been supportive at all times and accommodative.

My heartfelt thanks are due to all the Faculty and staff members specially Mr. Charanjeet Singh, Mr. Kuldeep Singh (Technicians) of the Mechanical Engineering Department, Thapar University Patiala for providing the necessary instrumentation facility for carrying out the research work.

I would also like to thank TEQIP- II for providing me grant and funds for carrying out research work.



Satnam Singh

ABSTRACT

In today's world refrigeration systems play a vital role to fulfill the human needs and a continuous research is being carried out by many researchers in order to improve the performance of these systems. Here, a such attempt has been made to improve the performance of the system. Our, present study on experimental investigations into the performance of nanorefrigerants (R134a + Al₂O₃, R134a + SiO₂) based refrigeration system, is conducted at the Mechanical Engineering Department, Thapar University, Patiala. The experimental setup is build up according to the national standards of India, and made to function under varying conditions. Performance of the refrigeration system depends upon the various factors like; performance of refrigeration system's components, nature and properties of the refrigerant being used, environmental conditions etc. During this research work, an attempt has been made to investigate the effect of nanoparticles on the performance of the refrigeration system. After deliberations & discussion it has been decided to use R134a as a base refrigerant which is commonly used refrigerant. But, it has been found that its refrigerant heat transfer capacity is limited and it also consumes more power when taken to refrigeration cycle. In addition to this, choice of a particular refrigerant also effects the temperature across condenser, evaporator of the refrigeration system. Selection of a refrigerant also effects the time taken to reach a particular temperature in the evaporator or freezing capacity. In order to make an improvement in its performance an experimental study has been conducted by using nanorefrigerant rather than the conventional refrigerant. Nanoparticles are injected along with the refrigerant R134a to increase the heat transfer capacity, to reduce the power consumption and there by to increase the performance of the system. Aluminium oxide (Al₂O₃) & Silicon oxide (SiO₂) nanoparticles of size (60-70) nm have been used in the refrigeration system. Two concentrations of nanoparticles

have been used. Data is collected for 11 LPH volume flow rate and for two heat fluxes in evaporator 25–26 °C and 35–36 °C. It has been found that addition of aluminium oxide and silicon oxide nanoparticles to the refrigerant results in an improvement in the thermo physical properties and heat transfer characteristics of the refrigeration system.

It has been observed that there is more temperature drop across the condenser for the nanorefrigerant (5.47% – 4.83%) compared to refrigerant R134a. Similarly, a gain of (6.89% – 8.08%) has been obtained for evaporator temperature. An improvement in COP is also observed during the investigations (1.17% – 8.40%). This is achieved under 25–26°C evaporator temperature load.

Similar improvements are also observed when refrigeration system is operated at 35–36 °C evaporator temperature load. A reduction in the power consumption (10.87% & 13.04%) along with faster cooling (from 40°C – 25°C) is also achieved when nanorefrigerants are used.

The experimental studies indicate that the refrigeration system with nano-refrigerant works normal like any conventional refrigeration system. Thus, aluminium oxide and silicon oxide (Al_2O_3 & SiO_2) nanoparticles can be used to improve the performance of a refrigeration system under investigated conditions.

Keywords:

Aluminum oxide nanoparticles, Silicon oxide nanoparticles, Nanorefrigerant, Thermal conductivity, Cooling Capacity, COP, Energy consumption.

CONTENTS

Chapters	Title	Page No.
	LIST OF FIGURES	
	LIST OT TABLES	
	NOMENCLATURE	
Chapter-1	INTRODUCTION	
1.1	Introduction Nanofluids	1
1.1.1	Properties of nanofluids	2
1.1.2	Nanofluids thermal conductivity	2
1.1.3	Particle volume fraction	3
1.1.4	Particle material	3
1.1.5	Base fluids	4
1.1.6	Particle size	4
1.1.7	Particle shape	4
1.2	Nanorefrigerants	5
Chapter-2	LITERATURE REVIEW	
2.1	Literature Review	6
Chapter-3	GAPS IN STUDY& OBJECTIVE	
3.1	Gaps in Study	15
3.2	Study Objectives	16
Chapter-4	NANOREFRIGERANT SELECTION AND MATERIAL PROPERTIES	
4.1	Materials for Nanoparticles and Base Fluids	17
4.2	Thermo physical properties of Base Refrigerant R134a	17
4.3	Material Characterization	19
4.3.1	X-ray Diffraction Analysis (XRD)	20
4.3.2	Scanning Electron Microscope (SEM)	21
4.3.4	Transmission Electron Microscopy (TEM)	21

Chapters	Title	Page No.
4.4	Specifications of Al ₂ O ₃ nanoparticle	22
4.5	Specifications of SiO ₂ nanoparticle	23
Chapter-5	EXPERIMENTAL SETUP AND METHODOLOGY	
5.1	Experimental Setup	24
5.2	Layout of vapor compression system	25
5.3	Experimental Methodology	26
5.4	Test Procedure	26
5.5	Charging of nanoparticles	27
5.6	Important Specifications	28
5.7	Experimental Setup & Components	28
5.7.1	Refrigeration Compressor	29
5.7.2	Refrigerant Flow Control Device	30
5.7.3	Condenser	31
5.7.4	Evaporator	32
5.7.5	Filter	34
5.7.6	Heating element	34
5.7.7	Pressure gauges	35
5.7.8	Rotameter	36
5.7.9	Refrigerant	37
5.7.10	Voltmeter	37
5.7.11	Ammeter	38
5.7.12	Energy meter	39
5.7.13	Digital temperature controller	40
5.7.14	Hand shut off valve	41
5.7.15	Temperature gauge (Mercury glass thermometers)	42

Chapters	Title	Page No.
5.7.16	Flexible charging line	43
5.7.17	Vacuum pump	43
5.8	Vapour compression refrigeration tools and materials	44
5.8.1	Tubing	44
5.8.2	Connecting tubing	44
5.8.3	Hand tools used	46
Chapter-6	RESULTS AND DISCUSSION	
6.1	Temperature drop in Condenser	48
6.2	Temperature gain in Evaporator	51
6.3	Coefficient of performance (COP)	54
6.4	Temperature-time graph	57
6.5	Cooling load temperature - time analysis for refrigerant R134a and SiO ₂ based nanorefrigerants at 11 LPH volume flow rate	61
6.6	Cooling load temperature - time analysis for refrigerant R134a and Al ₂ O ₃ based nanorefrigerants at 11 LPH volume flow rate	65
6.7	Cooling load temperature - time analysis at 11 LPH volume flow rate for refrigerant R134a, SiO ₂ and Al ₂ O ₃ nanoparticles based nanorefrigerants	67
6.8	Power consumption for cooling load temperature – time analysis	68
Chapter-7	CONCLUSION AND FUTURE SCOPE	
7.1	Conclusion	70
7.2	Challenges & Future scope	71
	REFERENCES	72
	APPENDIX	76

LIST OF FIGURES

Figure no.	Description	Page No.
4.1	XRD of Al ₂ O ₃ -alpha nanoparticles	20
4.2	SEM of Al ₂ O ₃ -alpha nanoparticles	21
4.3	SEM Analysis for silica nano powder	21
4.4	TEM Analysis for silica nano powder	22
5.1	Experimental setup	24
5.2	Line diagram of system	25
5.3	Layout of vapor compression system	25
5.4	Compressor, dimension and circuit diagram	29
5.5	Hand operated expansion valve	31
5.6	Finned static condenser	32
5.7	Coil type evaporator	34
5.8	Filter	34
5.9	Heating element	35
5.10	Pressure gauge	36
5.11	Glass tube type rotameter	36
5.12	Refrigerant	37
5.13	Voltmeter	38
5.14	Ammeter	39
5.15	Energy meter	40
5.16	Digital temperature controller	41
5.17	Relay switch	41
5.18	Hand shut off valve	42
5.19	Mercury glass thermometers	42

Figure no.	Description	Page No.
5.20	Flexible charging line	43
5.21	Vacuum pump	43
5.22	Copper Tubing	44
5.23	Flared connections	45
5.24	Flared type fittings	45
5.25	Flare nut ¼ inches	45
5.26	Brazed tubing	46
6.1	Temperature drop in condenser for nanorefrigerants at 11 LPH volume flow rate and heat flux at 25-26 °C	49
6.2	Temperature drop in condenser for nanorefrigerants at 11 LPH volume flow rate and heat flux at 35-36 °C	50
6.3	Temperature gain in evaporator for nanorefrigerants at 11 LPH volume flow rate and heat flux at 25-26 °C	52
6.4	Temperature gain in evaporator for nanorefrigerants at 11 LPH volume flow rate and heat flux at 35-36°C	53
6.5	COP comparison for nanorefrigerants at 11 LPH volume flow rate and heat flux at 25-26 °C	55
6.6	COP comparison for nanorefrigerants at 11 LPH volume flow rate and heat flux at 35-36 °C	56
6.7	Temperature-time graph for R134a refrigerant at 11 LPH volume flow rate	58
6.8	Temperature-time graph for refrigerant R134a+ SiO ₂ (0.25gm) at 11 LPH volume flow rate	59
6.9	Temperature-time graph for refrigerant R134a+ SiO ₂ (0.40gm) at 11 LPH volume flow rate	61
6.10	Temperature-time graph for refrigerant R134a and SiO ₂ based nanorefrigerants at 11 LPH volume flow rate	62
6.11	Temperature-time graph for refrigerant R134a+ Al ₂ O ₃ (0.25gm) at 11 LPH volume flow rate	63

Figure no.	Description	Page No.
6.12	Temperature-time graph for refrigerant R134a+ Al ₂ O ₃ (0.40gm) at 11 LPH volume flow rate	65
6.13	Temperature-time graph for refrigerant R134a and Al ₂ O ₃ based nanorefrigerants at 11 LPH volume flow rate	66
6.14	Temperature-time graph for nanorefrigerants at 11 LPH volume flow rate	67
6.15	Power consumption by nanorefrigerants for temperature drop from 40°C to 25°C	68

LIST OF TABLES

Table No.	Description	Page No.
4.1	Al ₂ O ₃ nanoparticles specifications	22
4.2	SiO ₂ nanoparticles specifications	23
5.1	Experimental Setup & Components	28
5.2	Compressor specifications	30
5.3	Condenser specifications	32
5.4	Evaporator specifications	33
5.5	Heater	35
5.6	Pressure gauge specifications	35
5.7	Refrigerant properties	37
5.8	Voltmeter	38
5.9	Ampere meter	39
5.10	Energy meter	40
5.11	Digital temperature controller	41
5.12	Hand tools used	46
6.1	COP, pressure and temperature for R134a refrigerant and nanorefrigerants at 11 LPH volume flow rate and heat flux at 25-26 °C	47
6.2	COP, pressure and temperature for R134a refrigerant and nanorefrigerants at 11 LPH volume flow rate and heat flux at 35-36 °C	48
6.3	Temperature –time data for refrigerant R134a at 11 LPH volume flow rate	57
6.4	Temperature –time data for refrigerant R134a+ SiO ₂ (0.25gm) at 11 LPH volume flow rate	59
6.5	Temperature –time data for refrigerant R134a+ SiO ₂ (0.40gm) at 11 LPH volume flow rate	60
6.6	Temperature –time data for refrigerant R134a + Al ₂ O ₃ (0.25gm) at 11 LPH volume flow rate	63
6.7	Temperature –time data for refrigerant R134a+Al ₂ O ₃ (0.40gm) at 11 LPH volume flow rate	64

NOMENCLATURE

COP	: Coefficient of performance
nm	: Nanometer
PHE	: Plate heat exchanger
CNT	: Carbon nanotubes
LPH	: Liter per hour
TEM	: Transmission Electron Microscope
SEM	: Scanning Electron Microscope
KW	: Kilowatt
EG	: Ethylene Glycol
POE	: Polyolester
Psi	: Pound square inch
ppm	: Parts per million
amp.	: Ampere
V	: Volts
Kg	: Kilogram
CC	: Centimeter cube
DI	: Deionized water
PAG	: Polyalkylene glycol
Hz	: Frequency
Cp	: Specific heat
CFD	: Computational fluid dynamics
K	: Temperature in Kelvin
km/hr	: Kilometer per hour
kWh	: Kilowatt hour energy consumed
kW	: Power consumption
m ³ /kg	: Specific volume
kg/m ³	: Density
wt%	: Concentration by weight
vol%	: Concentration by volume

L	: Volume in litre
P	: Pressure Kg/cm ²
T	: Temperature (°C)
Ecomp.	: Energy consumed by compressor
m ² /g	: Surface area per unit mass

INTRODUCTION

1.1 Introduction Nanofluids

In cooling and heating applications, thermo-physical properties of matter play a great role. It has been observed that the performance of any system mainly depends on the thermal conductivity, viscosity, specific heat and density of gasses and liquids which are used in system. Conventional fluids have poor heat transfer capacity and low thermal conductivity which limits its performance. Due to this, there is always a need to develop effective & efficient fluids capable to deal with high heat transfer rate. Small solid additives usually in micrometer are good option to enhance the thermal properties of fluids, but it has been found that these small solid additives poses number of problems like particle sedimentation, particle clogging, large pressure drop in the system, corrosion of components, etc (Maxwell et al., 1873). Investigations show that use of nanoparticles in conventional fluids is a good option and it also reduces the number of other problems because at nanometer the material behaves like colloidal solutions. Modern nanotechnology offers us many routes to prepare nanometer sized particles. It is possible to break down the limits of conventional solid particle suspensions by conceiving the concept of nanoparticle-fluid suspensions. These nanoparticle-fluid suspensions are termed nanofluids, obtained by mixing nanometer sized particles in a base fluid like, water, oil etc. Nanoparticles such as metallic oxides (Al_2O_3 , CuO , SiO_2), nitride ceramics (AlN , SiN), semiconductors (TiO_2 , SiC), carbide ceramics (SiC , TiC), metals (Cu , Ag), single, double or multi walled carbon nanotubes are used. Even at very low concentrations the nanofluid shows a good enhancement in the thermal conductivity and performance (Choi et al., 2001; Eastman et

al., 2001). With increase in concentration and temperature they show large improvement (Wang et al., 1999).

1.1.1 Properties of nanofluids

Like Conventional fluids, nanofluids have number of properties which explain its behavior like, particle size, particle shape, material, thermal conductivity etc. Also the stability of particles in base fluid is also a major concern. Researchers have been trying to find the unique properties of materials to make highly thermal conductive nanoparticles. Nanoparticles can be produced easily due to advancements in nanotechnology. Nanoparticles have high surface area to volume ratio, which help them to make stable suspensions. The cause of increase in thermal conductivity is due to the contact of solid particle with the liquid and gases. Thermal conductivity of nanoparticles is higher than base fluids due to which overall thermal conductivity of mixture increases. Due to the very small dimensions, the dispersed nanoparticles in base fluids can behave like a base fluid molecule in a suspension, which helps to reduce problems like particle clogging, sedimentation, corrosion etc. These properties make them suitable to prepare nanofluids. Viscosity of nanofluids is also an important concern. If amount of nanoparticles in base fluid is increased beyond certain limit (5%) then viscosity also increases which limits its performance & suitability for a particular application.

1.1.2 Nanofluids thermal conductivity

The use of nanoparticle is decided mainly on the basis of improved value of thermal conductivity. There are both theoretical as well as practical models to explain the rise in the thermal conductivity of nanofluids. But research is still going on to find the best ways to explain the increased value of thermal conductivity. The main focus is to find the right concentration of nanoparticles so that thermal conductivity gets improved. Nanofluids show superior results over

the base fluids. Phenomenon like boiling and convection are being studied by many researchers to find the coefficient of heat transfer so that improvement can be made in this field. Also the shape and size plays an important role in the thermal conductivity enhancement. Higher is the surface area higher is the value for thermal conductivity of nanoparticles.

1.1.3 Particle volume fraction

Particle volume fraction represents the amount of nanoparticles in the base fluids. All experiments and studies on nanofluids are based on this. This effects the viscosity of the base fluid and thermal conductivity. There are many studies that have been performed to see the effect of particle volume fraction on the thermal conductivity of nanofluids. An enhancement up to 32.4% was observed in the effective thermal conductivity of nanofluids for a volume fraction of about 4.3% of Al_2O_3 nanoparticles (Masuda et al., 1993). Studied done by Lee et al. (1999) at the room temperature to calculate the thermal conductivity of water as well as ethylene glycol (EG) based nanofluids consisting of Al_2O_3 (38.5nm) and CuO (23.6nm) nanoparticles show an enhancement around 20% in the thermal conductivity for 4% volume fraction of CuO in CuO/EG nanofluid.

1.1.4 Particle material

Particle material is the main property which decides the thermal conductivity of the nanofluids. CuO is more conducting than Al_2O_3 nanoparticle. Investigations also shows that water and EG based nanofluids consisting of Ag_2Al as well as Ag_2Cu nanoparticles suspensions, Ag_2Al nanoparticles shows slightly more enhancement in the value of thermal conduction than Ag_2Cu nanoparticle suspensions (Chopkar et al., 2008). This was explained as due to the higher thermal conductivity of Ag_2Al nanoparticles. In the base fluids also CNT shows high thermal

conductivity & heat transfer coefficient as compared to base fluids .This is due to high thermal conductivity of CNT and larger surface area (Choi et al., 2001).

1.1.5 Base fluids

According to the conventional effective medium theory (Maxwell, 1873), the less is the thermal conductivity of base fluid more is the thermal conductivity ratio when we use nanoparticles. Ethylene glycol has less thermal conductivity than water and engine based fluids. EG based nanofluids show high thermal conductivity ratio as compared to others. Engine oil shows some what lower thermal conductivity ratio than ethylene glycol. Water and pump oil shows even a smaller ratio of thermal conductivity rise. Also, the base fluids should be such that they should be able to carry the nanoparticles without sedimentation. Some nanoparticles are compatible with some fluids while others do not. So selection of the nanoparticles & base fluid is also an important step in order to carry out the investigation of the nanofluids.

1.1.6 Particle size

The advent of nanofluids offers Small size of nanoparticle from (5-500) nm size, with different shapes and materials. Thermal conductivity of nanofluids also depends on the particle size; smaller size particles have more surface area which causes more contact with base fluid. Viscosity is also particle size dependent. Larger the size of the nanoparticle more is the viscosity. In all these cases it has been found that the effective thermal conductivity of a nanofluid increases with decreasing nanoparticle size. But in some cases it is not true, conflicting results also have been reported.

1.1.7 Particle shape

Nanoparticles are available in different shapes like spherical, cylindrical etc. The aspect ratio of cylindrical nanoparticles is more than the spherical nanoparticles. It has been reported in

literature that nanofluids with cylindrical nanoparticles shows higher thermal conductivity than other particle nanofluids. In cylindrical shapes heat transfer is along the wall of the tube. For example a volume fraction of 4.2% cylindrical particles show 22.9% higher conductivity than the spherical particles (Xie et al., 2002a). A general observation is that nanofluids with nanotubes show high thermal conductivity because of heat transfer along the tube length, but at the same time the nanofluids with cylindrical particle suspension need higher pumping power due to increased value of viscosity.

1.2 Nanorefrigerants

Recently, some studies on the use of nanoparticles in refrigeration systems have been conducted & which improve heat transfer, characteristics of the system. Nanoparticles used with refrigerant as a base fluid are called nanorefrigerants. It has been observed that domestic refrigerator with R134a as refrigerant and a mixture of mineral oil and TiO_2 as the lubricant shows an improvement in performance (Bi et al., 2007). Jwo et al. (2009) mixed mineral lubricant with Al_2O_3 nanoparticles to improve the lubrication and heat-transfer performance. This study showed that R-134a and 0.1 wt % Al_2O_3 nanoparticles were optimal. Bi et al. (2011) used a domestic refrigerator of 228 L with reciprocating compressor for experimental study. TiO_2 -R600a nano-refrigerant was used as working fluid. It has been observed that there are number of nanorefrigerants that can be used to improve the performance of refrigeration systems.

LITERATURE REVIEW

2.1 Literature Review: In the past a large amount of experimental and theoretical research has been done to investigate the thermo-physical behavior of nanofluids and nanorefrigerants. In these investigations it has been shown that thermal conductivity enhancement is obtained with addition of small concentrations of nanoparticles in the basefluid. Suspension of these nanoparticles in basefluid leads to higher value of thermal conductivity. In the present study, prior to the research work, an extensive review of the published works in the field of nanorefrigerants technology with an emphasis on the effects of different factors like particle size, particle concentration, nanoparticle material, etc. that effects the nanorefrigerant working in the vapour compression refrigeration system has been presented.

Choi S.U.S et al. (1995) suggested the concept of nanofluids by suspending metallic or nonmetallic particles. Recently some studies have been reported on nanoparticles in refrigeration systems because of its capability to improve heat transfer characteristics, hence efficiency enhancement.

Kumar R.R et al. (2013) investigated the effect of aluminium oxide based nano-lubricant on the COP of the system and freezing capacity of the system. The experimental set up was build as per Indian standards. Refrigerants like R12, R22, R600, R600a and R134a were used as a refrigerant. The performance of the system depends upon the thermo-physical properties of the refrigerant. The addition of nanoparticles to the refrigerant results in improvement in the thermo- physical properties thereby improving the performance of the refrigeration system. The experimental studies indicate that the refrigeration system with nanorefrigerant works normally.

There was increase in the COP of the system by 19.6 %. Mineral oil with alumina nanoparticles oil mixture was investigated and it was found that there is an increase in freezing capacity and reduction in power consumption by 11.5 % as compared to polyester. Aluminium oxide based nano-lubricant in refrigeration system was found working satisfactorily.

Mahbubul I.M et al. (2012) studied the volumetric and temperature effects over viscosity of R123-TiO₂ nanorefrigerants for 5°C to 20°C temperatures and up to 2 % volume concentration of nanoparticles. The effect of pressure drop with the increase in viscosity has also been investigated. Based on the analysis it was found that viscosity of nanorefrigerant increases accordingly with the increase of nanoparticle volume concentrations and decreases with the rise in temperature. Furthermore, pressure drop increases significantly with the intensification of volume concentrations. Therefore low volume concentrations of nanorefrigerant are suggested for better performance of a refrigeration system.

Bi et al. (2007) have experimented on a domestic refrigerator with R134a as refrigerant and a mixture of mineral oil and TiO₂ was used as the lubricant. It was found that the refrigeration system with the above combination works normally and efficiently and the energy consumption reduces by 21.2% as compared with R134a/POE oil system.

Jwo C.S et al. (2009) had mixed mineral lubricant with Al₂O₃ nanoparticles to improve the lubrication and heat-transfer performance. This study showed that R134a + 0.1 wt % Al₂O₃ nanoparticles were optimal for best performance. Under these conditions, the power consumption was reduced by about 2.4%, and the coefficient of performance was increased by 4.4%.

Kang Y.T et al. (2012) measured the thermal conductivity of the Al₂O₃ nanofluids using the transient hot-wires method (THWM). The experimental uncertainties in repeatability were

obtained as 1.95% for DI water and 1.34% for pure methanol, respectively. The results show that the dispersed nanoparticles can always enhance the thermal conductivity of the base fluid and the highest enhancement observed was 6.3% in the concentration of 0.1% (vol.) of Al_2O_3 nanoparticles, 40% (vol.) of CH_3OH and 10% (wt.) of NaCl at 293.15 K. In addition, the zeta potential, visualization and Tyndall effect were also investigated to discuss the stability of nanofluids.

Subramani N et al. (2011) studies indicated that the refrigeration system with nanorefrigerant works normally. It was found that the freezing capacity is higher and the power consumption reduces by 25% when POE oil is replaced by a mixture of mineral oil and alumina nanoparticles. Calculations showed that the enhancement factor in the evaporator is 1.53 when nanorefrigerants were used instead of pure refrigerant.

Kumar S.D et al. (2012) did experimental work on nanorefrigerant .Nanoparticle Al_2O_3 -PAG oil in R134a vapour compression refrigeration system. An experimental setup was designed and fabricated. The system performance was investigated using energy consumption test and freeze capacity test. The results indicated that Al_2O_3 nanorefrigerant works normally and safely in the refrigeration system. The performance of refrigeration system was better than pure lubricant with R134a working fluid, a 10.32% less energy was consumed when 0.2% volume of the concentration used in the system. The results indicated that heat transfer coefficient increases with the usage of nanoparticle Al_2O_3 . Thus, using Al_2O_3 nanorefrigerant in refrigeration system is found to be feasible and works normally.

Gupta H.K et al. (2012) according to them advancements in nanotechnology have originated the new emerging heat transfer fluids called nanofluids. Nanofluids are prepared by dispersing and stably suspending nanometer sized solid particles in

conventional heat transfer fluids. Past researches have shown that a very small amount of suspending nanoparticles have the potential to enhance the thermo physical and transport properties of the base fluid. Due to improved properties, a better heat transfer performance is obtained in many energy consuming and heat transfer devices as compared to traditional fluids which open the door for a new field of scientific research and innovative applications.

Wang K.J et al. (2006) carried out an experiment and studied boiling heat transfer characteristics of refrigerant R22 with Al₂O₃ nanoparticles. The study showed improvement in heat transfer properties and reduced bubble size near heat transfer area.

Peng H et al. (2011) investigated experimentally influence of refrigerant-based nanofluids composition and heating condition on the migration of nanoparticles during pool boiling. The nanoparticles include Cu (average diameters of 20, 50 and 80 nm), Al and Al₂O₃ (average diameters of 20 nm), and CuO (average diameter of 40 nm). The refrigerants include R113, R141b and n-pentane. The mass fraction of lubricating oil RB68EP is from 0 to 10 wt%, the heat flux is from (10 to 100) kW/m² and the initial liquid-level height was from 1.3 to 3.4 cm. The experimental results showed that a migration ratio of nanoparticles during the pool boiling of refrigerant-based nanofluid increases with the decrease of nanoparticle density, nanoparticle size, dynamic viscosity of refrigerant, mass fraction of lubricating oil or heat flux; while increases with the increase of liquid-phase density of refrigerant or initial liquid-level height.

Hafez E.A et al. (2011) used CuO-R134a in the vapour compression system and evaporating heat transfer coefficient was experimentally investigated. Measurements were taken for heat flux ranged from 10 to 40 kW/m², using CuO nanoparticles with different concentrations (0, 0.1, 0.2, 0.3, 0.4, 0.5, 0.55, 0.6, 0.8 and 1%) and nanoparticles size was from 15 to 70 nm. There

is increase in heat transfer coefficient up to 0.55% in the investigated concentration range and then decreases for all values of heat flux. With nanoparticle size up to 25 nm heat transfer coefficient increases than decrease with the increase in size of nanoparticle.

Pruzaesky F.C et al. (2010) studied numerically the use of nanofluids as secondary coolants in vapor compression refrigeration systems. A simulation model for a liquid-to-water heat pump, with reciprocating compressor and double-tube condenser and evaporator was studied. The multi-zone method was employed in the modeling of the heat exchangers. The water based nanofluid was supposed to flow through the inner circular section of the evaporator, while the refrigerant was left to the annular passage. A computational program was developed to solve the resulting non-linear system of algebraic equations. Different nanoparticles (Cu, Al₂O₃, CuO and TiO₂) were studied for different volume fraction and particle diameters. Simulation results have shown that, for a given refrigerating capacity, evaporator area and refrigerant-side with the increase in volume fraction of nanoparticles pressure drop are reduced. Also, nanofluid-side pressure drop and, consequently, pumping power, increase with nanoparticle volume fraction and decrease with nanoparticle size. Results show a decrease in evaporator area when we use nanofluid as compared to the conventional fluid (H₂O).

Ding G (2007) simulation has been widely used for performance prediction and optimum design of refrigeration systems. A brief review on history of simulation for vapour-compression refrigeration systems is done. The models for evaporator, condenser, compressor, capillary tube and envelop structure are summarized. Some developing simulation techniques, including implicit regression and explicit calculation method for refrigerant thermodynamic properties, model-based intelligent simulation methodology and graph-theory based simulation method, are presented. Prospective methods for future simulation of refrigeration systems, such as noise-

field simulation, simulation with knowledge engineering methodology and calculation methods for nanofluid properties are introduced briefly.

Pantzali M.N et al. (2009) development of plate heat exchangers (PHE) with modulated surfaces has been mainly driven by the need for compact, high performance, yet small in size and light weight equipment. The type of flow inside PHE channels augments heat transfer, due to flow separation and reattachment, while the complexity induced by the modulations significantly increases the friction losses. Since the flow passages in such PHEs are complex in geometry and of small dimensions, it is very difficult to conduct accurate measurements of the operation parameters (e.g. temperature, pressure and velocity fields). Thus, CFD simulation, which is considered an effective and reliable tool, can be used to estimate momentum and heat transfer rates in this type of process equipment.

During the last decade and in order to enhance the thermal conductivity of the working fluids in heat transfer equipment, nanometer-sized solid-particle suspensions in common fluids (e.g. water, ethylene glycol), called nanofluids, have been employed. These suspensions exhibit a significant increase in the thermal conductivity compared to the base fluid while problems of sedimentation can be encountered. Experimental work in the convective heat transfer of nanofluids is still quite scarce, so further investigations are needed.

Loaiza J.C.V et al. (2010) studied the use of nanofluids as secondary coolants in vapor compression refrigeration systems numerically with a simulation model for a liquid-to-water heat pump, using reciprocating compressor and double-tube condenser and evaporator. The simulation program was run for a small capacity system operating with four different water-based nanofluids, Cu, Al₂O₃, CuO and TiO₂ and volume fraction ranged from 1% to 5% and particle size from 10 to 50 nm. It was observed that greatest reductions in evaporator area were

obtained with Cu+H₂O nanofluid, flowing with large volume fractions and lower particle diameters followed by TiO₂ and Al₂O₃ results increase in COP of the system.

Mamut E (2006), the paper presents the results of a research project regarding the characterization of the thermal conductivity of nanofluids like water + Cu nanoparticles. The experimental results are compared with theoretical simulations based on the assumptions regarding the heat and mass transfer.

Bozorgan N et al. (2012) studied numerically the application of CuO-water nanofluid with 20 nm size particle and volume concentrations up to 2% in a radiator of Chevrolet Suburban diesel engine under turbulent flow conditions. They measured the local and overall heat transfer coefficient in the radiator and also measure the pressure drop and pumping power. In the present study, the effects of the automotive speed and Reynolds number of the nanofluid in the different volume concentrations on the radiator performance are also investigated. The results show that for CuO-water nanofluid at 2% volume concentration circulating through the flat tubes with Reynolds No 6000 while the automotive speed is 70 km/hr, the overall heat transfer coefficient and pumping power are approximately 10% and 23.8% more than that of base fluid for given conditions, respectively.

Clancy E.V et al. (2012) proposed a new design, where the heat transfer of a vapour compression system was increased by increasing the thermal heat transfer properties of the refrigerant using nanoparticles. Nanoparticles were mixed with refrigerant at inlet of the condenser and removed at outlet of condenser, so by this means heat transfer rate was accelerated in condenser. This research recommended a less than 10% (wt.) of nanoparticles in the fluid. Moreover, the condenser efficiency can be enhanced to improve the performance of the system.

Eiyad A.N et al. (2008) presented the numerical investigation of nanofluids heat transfer with backward facing step. Different types of nanoparticles in different volume fractions were used in base fluid. To solve the momentum and energy equation finite volume technique was used. Nusselt number at the top and the bottom walls of the BFS was obtained. For Cu nanoparticles, there was increment in Nusselt number. Nanoparticles which have high thermal conductivity show more enhancements in Nusselt number outside the recirculation zones like Ag, Cu. But in recirculation zone, low thermal conductivity nanoparticles shows a better heat transfer. There is increase in Nusselt number for increases in volume fractions for whole range of Reynolds number.

Bi et al. (2011) used a domestic refrigerator of 228 L with reciprocating compressor for experimental study. As a working fluid he uses TiO₂-R600a. The results showed reduction in temperature of lower food and frozen food storage compartment with the nanorefrigerant compared to pure R600a. Using 0.1 g/L nanoparticles energy saving was 5.94%, whereas with 0.5 g/L nanoparticles energy saving was 9.6%.

Parise J.A.R et al. (2012) developed the simulation model using nanofluids as condenser coolants for the performance prediction of a vapor compression heat pump. It consists of a liquid-to-liquid heat pump, with reciprocating compressor, thermostatic expansion valve and counter-flow double-tube condenser and evaporator. The compressor is specified by the swept volume, shaft speed and isentropic and volumetric efficiencies curves, and the expansion device, by the evaporator superheat. The condenser is divided into three zones, de-superheating, condensing and sub cooling. The evaporator is also divided into the boiling and superheating zones. The heat exchangers specified by their geometry like length of the tube. Mass flow rates and inlet states were also added in the equations. This is solved by a computational model and

we got the cycle overall thermal performance, as well as condensing and evaporating pressures and the thermodynamic states of refrigerant. Results were obtained for the simulation of a 19 kW capacity water-to-water/ (H₂O-Cu nanofluid) heat pump. For a volume fraction of 2% there is increase of heat transfer coefficient by 5.4%.

Pawel K.P et al. (2005) conducted studies on nanofluids and it is found that there is significant increase in the thermal conductivity of nanofluid compared to the base fluid. They also found that addition of nanoparticles results in significant increase in the critical heat flux.

Coumaressin T et al. (2014) investigated experimentally that the CuO nanoparticle with R134a refrigerant can be used as an excellent refrigerant to improve the heat transfer characteristics in a refrigeration system. A successful model has been designed and the basic theoretical heat transfer analysis of the refrigeration system has been done. Successful mesh has been designed for the test section using GAMBIT software and Computational Fluid Dynamics (CFD) Heat Transfer analysis for the designed test Section has been successfully performed using FLUENT software. It has been observed that evaporating heat transfer coefficient increases with the usage of nano CuO.

GAPS IN STUDY & OBJECTIVES

Literature review shows that research work is being reported on the nanofluid's thermal conductivity, its properties, effect of particle volume fraction, particle material, base fluid, particle size, particle Shape etc. Use of nanofluids in different areas was also a point of discussion. Nanofluid's application in the area of refrigeration and air conditioning is also an emerging field where lot of investigation is required.

3.1 Gaps in Study

Researchers have been trying different concentrations of nanoparticles in the base fluids in order to investigate their performance. But following are the points which helped me to take my thesis work on nanorefrigerants based refrigeration system are as under:

- (i) A limited work has been reported on the nanorefrigerants and its effect on the performance of vapour compression cycle
- (ii) There is a range of conventional refrigerants which are used in vapour compression cycle, but the conventional refrigerants suffer from poor thermal performance
- (iii) Properties of the refrigerant effect the performance of the refrigeration system and addition of nanoparticles in base fluid improves its properties & performance. It is believed that nanoparticles based refrigerant so called nanorefrigerant will also improve the performance of refrigeration system
- (iv) A limited work has been reported on application of nanofluids and in this direction
- (v) It has also been observed that nanorefrigerant also effect the performance of compressor, its power consumption etc., which is also a matter of investigation

3.2 Study Objectives

After an extensive literature survey it has been decided to investigate the performance of Al_2O_3 , SiO_2 based nanorefrigerant in the vapour compression cycle. Following are the parameters which are set as thesis's objectives and undertaken for investigation.

- (i) COP of refrigeration system
- (ii) Power consumption, pressure drop in refrigeration system
- (iii) Effect of volumetric concentration of nanoparticles
- (iv) Study the performance under varying mass flow rates
- (v) Time required to achieving a desired temperature/freezing capacity of the system
- (vi) Temperature drop across the condenser, temperature gain across the evaporator
- (vii) Pressure drop across evaporator & condenser
- (viii) Effect of mixed nanoparticles

NANOREFRIGERANT SELECTION AND MATERIAL PROPERTIES

4.1 Materials for Nanoparticles and Base Fluids

1) Nanoparticle materials include:

- Oxide ceramics – Al_2O_3 , ZnO , SiO_2
- Metal carbides – SiC
- Nitrides – AlN , SiN
- Metals – Al , Zu
- Nonmetals – Graphite, carbon nanotubes
- Layered – $\text{Al} + \text{Al}_2\text{O}_3$, $\text{Cu} + \text{C}$
- PCM – S/S

2) Base fluids include:

- Water
- Ethylene or tri-ethylene-glycols and other coolants
- Oil and other lubricants
- Bio-fluids
- Polymer solutions
- Other common fluids
- Refrigerants like R12, R22, R600, R600a and R134a etc.

4.2 Thermo physical properties of Base Refrigerant R134a

Refrigerant R134a is commonly used as working fluid in domestic vapour compression refrigeration system. It is a low pressure refrigerant. Refrigerant R134a is a haloalkane

refrigerant with thermodynamic properties similar to refrigerant R-12 but with a smaller amount ozone depletion potential. Its numerical designation is R134a or Isobutene. Its chemical formula is $(\text{CH}_2\text{FCF}_3)$. Thermo-physical properties plays great role in the system design. These are presented below.

Gas properties

- Molecular weight : 102.03 g/mol

1) Solid phase

Melting point at 1.013 bar is -101°C

2) Liquid phase

- Liquid density at 1.013 bar and 25°C is 1206 kg/m^3
- Boiling point at 1.013 bar is -26.55°C
- Latent heat of vaporization at 1.013 bar at boiling point is 215.9 kJ/kg
- Vapor pressure at 20°C is 5.7 bar
- Vapor pressure at 5°C is 3.5 bar
- Vapor pressure at 15°C is 4.9 bar
- Vapor pressure at 50°C is 13.2 bar

3) Critical point

- Critical temperature is 100.95°C
- Critical pressure is 40.6 bar
- Critical density is 512 kg/m^3

4) Triple point

- Triple point temperature is -103.3°C

5) Gaseous phase

- Gas density at 1.013 bar at boiling point is 5.28 kg/m³
- Gas density at 1.013 bar and 15°C is 4.25 kg/m³
- Compressibility Factor (Z) at 1.013 bar and 15°C is 1
- Specific gravity is 3.25
- Specific volume at 1.013 bar and 15°C is 0.235 m³/ kg
- Heat capacity (C_p) at constant pressure 1.013 bar and 25°C is 0.08754 kJ/(mol K)

4.3 Material Characterization

Material Characterization of materials refers to the use of some methods to probe into the internal structure and properties of a material. Analysis techniques are used simply to magnify the specimen and to visualize its internal structure.

Magnification and internal visualization are done in microscopes, such as:

- (i) Optical Microscope
- (ii) Scanning Electron Microscope (SEM)
- (iii) Transmission Electron Microscope (TEM)
- (iv) Field Ion Microscope (FIM)
- (v) Scanning Tunneling Microscope (STM)
- (vi) Atomic Force Microscope (AFM)
- (vii) X-ray Diffraction Topography (XRT)

Elemental analysis of the specimen can also be done with the help of these methods

- (i) Energy-Dispersive X-ray Spectroscopy (EDX)
- (ii) Wavelength Dispersive X-ray Spectroscopy (WDX)
- (iii) X-ray Diffraction (XRD)

- (iv) Mass Spectrometry
- (v) Secondary Ion Mass Spectrometry (SIMS)
- (vi) Electron Energy Loss Spectroscopy (EELS)
- (vii) Auger Electron Spectroscopy

Materials Characterization is done for

- (i) Precisely measuring the physical and chemical properties of materials
- (ii) Accurately determining the atomic level and microscopic level structure of a material
- (iii) To study the relationships between Properties of materials
- (iv) To see the Structures and Microstructures of materials
- (v) To determine the processing used to make the materials

4.3.1 X-ray Diffraction Analysis (XRD): X-ray powder diffraction is a rapid analytical technique primarily used for phase identification of a crystalline material and can provide information on unit cell dimensions. The analyzed material is finely ground, homogenized and average bulk composition is determined.

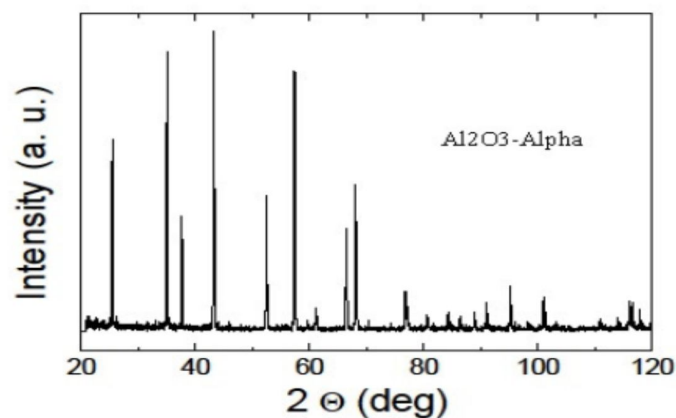


Fig.4.1: XRD of Al₂O₃-alpha nanoparticles

4.3.2 Scanning Electron Microscope (SEM): SEM is standardized method for imaging and measuring the dimensions of nanometer and micrometer size particles because of high imaging speed and high resolution of SEM. Scanning electron microscope uses electron to form an image. The electrons interact with the atoms in the sample, producing various signals that can be detected and that contain information about the sample's surface topography and composition. The SEM has large depth of field, which allows more of a specimen to be in focus at one time.

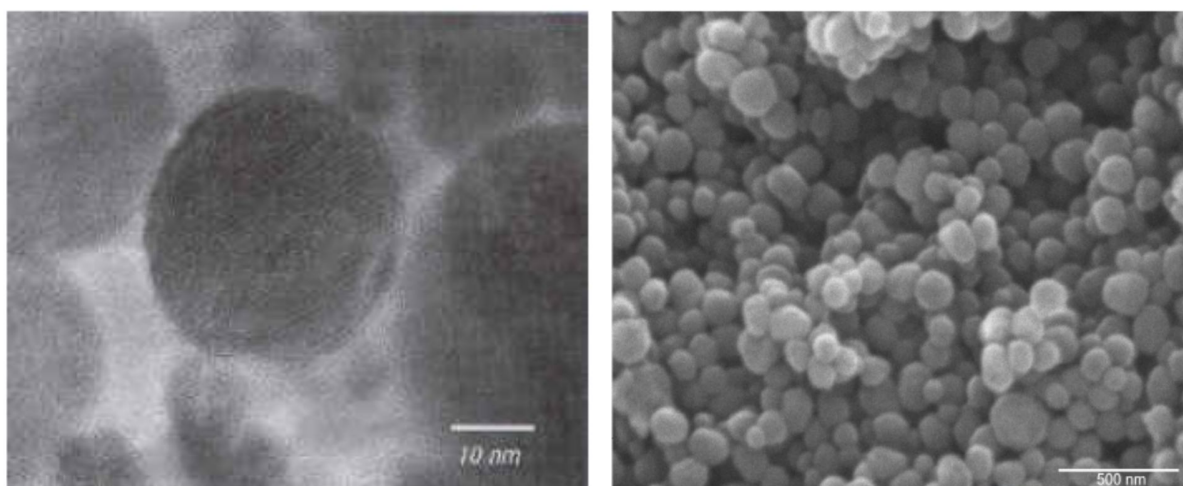


Fig.4.2: SEM of Al₂O₃-alpha nanoparticles **Fig.4.3: SEM Analysis for silica nano powder**

4.3.3 Transmission Electron Microscopy (TEM): Transmission electron microscopy (TEM) is also a standardized method for imaging and measurements of dimension of nano and micro size structures due to their high imaging speed and high resolution. It is a microscopy technique in which a beam of electrons is transmitted through an ultra-thin specimen, interacting with the specimen as it passes through an image is formed from the interaction of the electrons transmitted through the specimen. The image is magnified and focused onto an imaging device, such as a fluorescent screen.

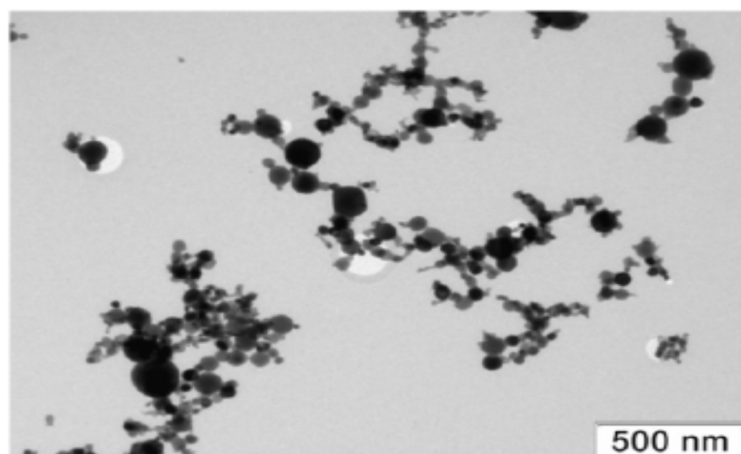


Fig.4.4: TEM Analysis for silica nano powder

4.4 Specifications of Al₂O₃ nanoparticle

Product Name	Alumina powder nano grade
Color	White
Crystal Form	Alpha
PH Value	6.6
SSA m ² /g	15-20
Particle Size	<80nm
Al ₂ O ₃ content	99.99%
Si	10.8 ppm
Na	9.01 ppm
Fe	9.75 ppm
Cu	12 ppm
Ti	0.86 ppm
K	10.6 ppm
Mn	0.72 ppm

Table 4.1: Al₂O₃ nanoparticles specifications

4.5 Specifications of SiO₂ nanoparticle

Product Name	Silicon oxide nano powder
Purity	98%
APS	60-70nm
SSA	110-120 m ² /g
Color	White
Bulk Density	<0.10 g/cm ³
True Density	2.4g/cm ³
Ultraviolet Reflectivity	>75%.
SiO ₂	10ppm
Al	10ppm
Fe	30ppm
Sr	40ppm
Ca	20ppm
Mg	20ppm
Cl	10ppm
Cr	20ppm

Table 4.2: SiO₂ nanoparticles specifications

EXPERIMENTAL SETUP AND METHODOLOGY

5.1 Experimental Setup

This section provides a detailed description on the facilities developed for conducting the experimental work on a domestic refrigerator. The technique used for charging nanoparticles and evacuation of the system is also discussed here. A detailed report on this facility development is as follows.

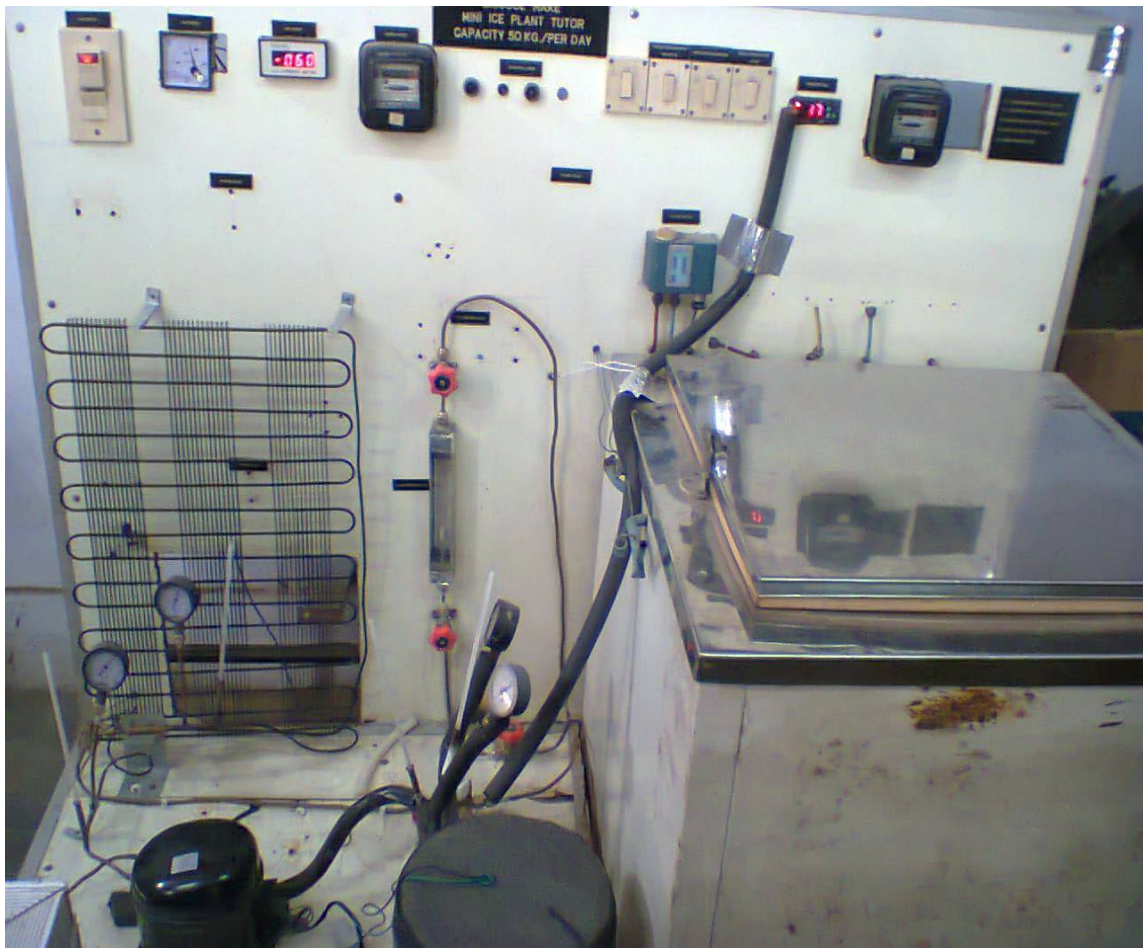


Fig.5.1 Experimental setup

Figure 5.1 shows the actual setup for vapour compression domestic refrigerator in which R134a refrigerant is used as working fluid along with the nanoparticles.

5.2 Layout of vapor compression system

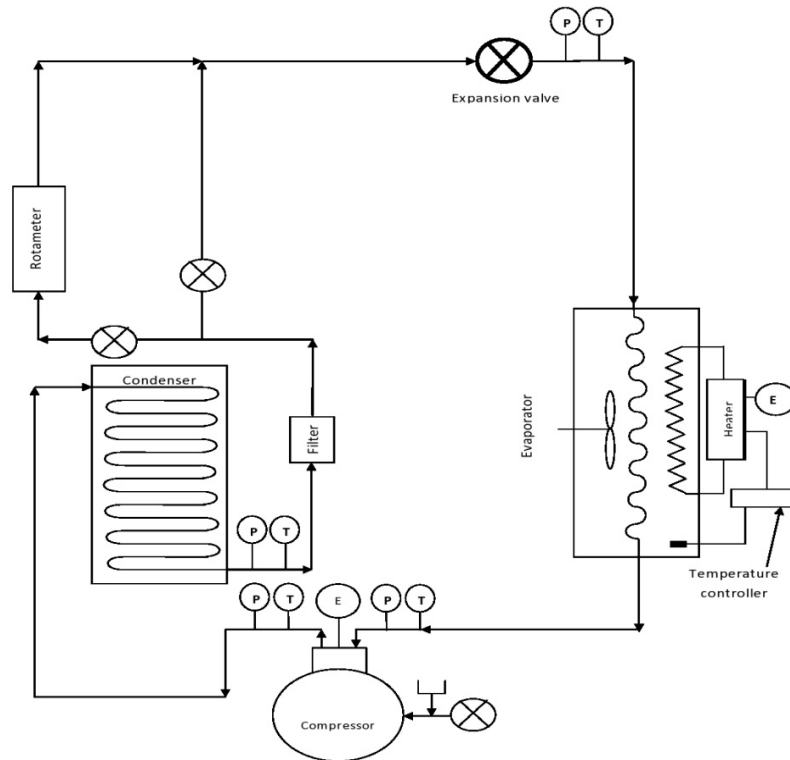


Fig.5.2: Line diagram of system

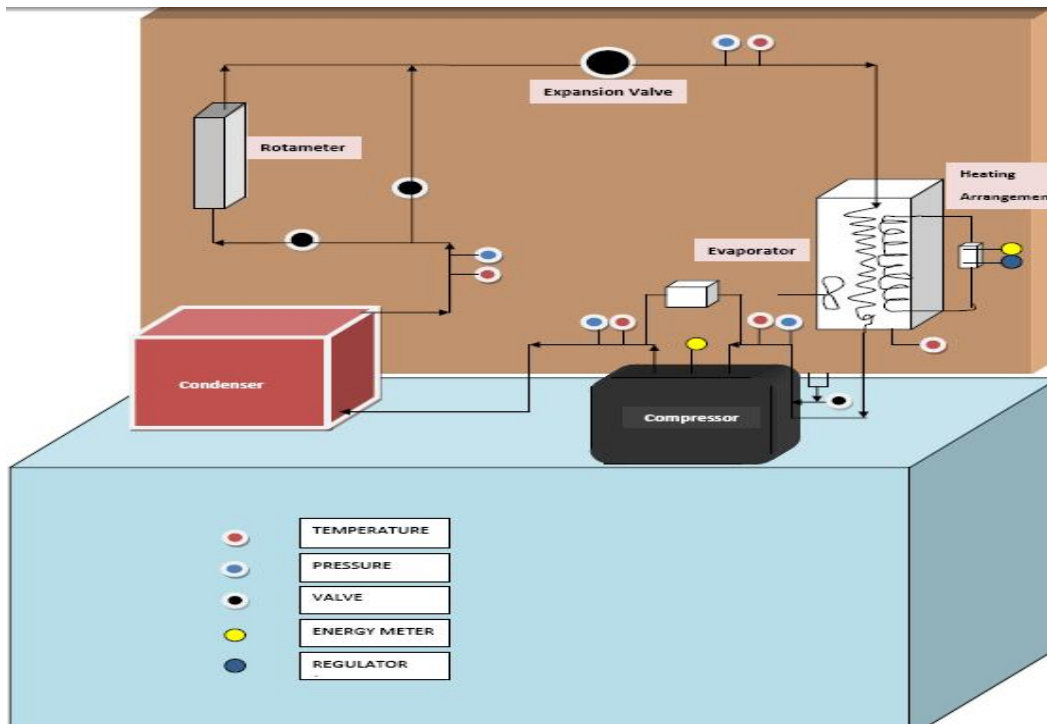


Fig.5.3: Layout of vapor compression system

5.3 Experimental Methodology

The temperature of the refrigerant at inlet/outlet of each component of the refrigerator is measured with thermometers. Temperature measurement is necessary across each component of the system in order to investigate the performance. Similarly pressure measurements are also taken across different components of the refrigeration system. The Pressure gauges are fitted at the inlet and outlet of the compressor and expansion valve. The pressure gauges are fitted with the T-joint and then brazed with the tube to measure the pressure at desired position. A power meter is connected with compressor and heater to measure the power and energy consumption. Firstly, performance of the system is investigated with pure refrigerant R134a. Then nanoparticles are injected in the refrigerator through charging line for the refrigerant. Then performance is investigated with the Al₂O₃ nanoparticle and SiO₂ nanoparticle. Volumetric concentration of nanoparticles, mass flow rate of refrigerant are the key parameters which varied during experimentation.

5.4 Test Procedure

The experimental test facility is developed with reference to the domestic refrigerator. The test rig is placed in a constant room temperature with proper insulation. The fluctuation of ambient temperature is $\pm 2^\circ\text{C}$ and the air velocity in room is found to be 0.1m/s. Evaporator of the system is dipped in 10.5 liter water and it maintained at constant temperatures (25-26 °C) and (35-36 °C). All readings are taken on one volume flow rate (11 LPH). First data is collected for pure refrigerant R134a and then nanorefrigerant is introduced with two mass fractions 0.25% (wt.) of refrigerant charged mass and again 0.40% (wt.) of refrigerant charged mass. The charged mass of the gas is 100 gm. Experiments are carried out with 60-70 nm nanoparticle size. Tests are performed to study power consumption, COP, time taken for temperature drop from 40°C to 25°C at 11LPH volume flow rate, temperature drop in condenser, temperature gain in

evaporator, temperature at all salient points. The temperature of the refrigerant at inlet and outlet of each component is measured with mercury thermometers.

Firstly system is evacuated to remove moisture, as moisture may combine with refrigerant and affect the thermo-physical properties. Moreover it produce highly corrosive compound, hence produce pitting and damage to valves and compressor cylinder walls. It also leads to choking of expansion device which may cause improper expansion or blockage of flow. So to remove moisture system was evacuated by creating vacuum with the help of external air compressor. After evacuation system is charged with refrigerant R134a and amount is 100gm. Now the system is switched on and steady state is achieved in approximately one hour. After steady state, readings of pressures and temperatures at compressor suction and discharge, after condenser and after expansion, were taken with 15 minute interval. Ambient temperature is also noted regularly. At the start and at the end of the experiment readings for energy meters for compressor and heater are also noted. Data is collected to find the COP of the system. Same procedure is adopted for refrigerant R134a, nanorefrigerant R134a + SiO₂ (60-70 nm) 0.25% mass fraction, nanorefrigerant R134a + SiO₂ (60-70 nm) 0.40% mass fraction and nanorefrigerant R134a + Al₂O₃ (60-70 nm) 0.25% mass fraction, nanorefrigerant R134a + Al₂O₃ (60-70 nm) 0.40% mass fraction. After investigating the different parameters, performance of the refrigeration system is evaluated.

5.5 Charging of nanoparticles

Measured & required quantity of SiO₂ and Al₂O₃ is taken and weighed in digital weighing machine. After this with the help of vacuum pump air from the system is removed. Nanoparticles are placed in charging line, before charging the refrigerant R134a the line is purged to remove any air in the charging line. Then R134a refrigerant is made to charge the

system through the charging line which carries the nanoparticles along with it. Thus it is understood that the system is charged with nanorefrigerant.

5.6 Important Specifications

- Refrigerant charged mass – 100 gm
- Concentration of nanoparticles – 0.25-0.40 gm
- Size of nanoparticles – Al₂O₃ (60-70nm), SiO₂ (60-70nm)

5.7 Experimental Setup & Components

S. No.	Component	Qty.	Specification
1	Compressor (R134a)	1	165 liter
2	Expansion device (Manual)	1	as per compressor
3	Condenser	1	as per compressor
4	Evaporator	1	as per compressor
5	Filter	1	Without silica gel
6	Heating element	1	230 W
7	Pressure gauge	4	Two low ,Two high pressure
8	Rotameter	1	4-40 LPH
9	Refrigerant	1000 grams.	99.9% pure R134a
10	Volt meter	1	0-300 Volt
11	Ampere meter	1	0-15Amp.
12	Energy meter	2	
13	Digital temperature controller	1	
14	Hand shut valve	4	For ¼ inch pipe
15	Temperature gauge (Thermometer)	5	Mercury glass thermometer
16	Flexible charging Line	1	
17	Vacuum pump	1	

Table 5.1: Experimental Setup & Components

5.7.1 Refrigeration Compressor: Compressor is an integral part of any refrigeration system.

To raise the pressure and temperature of the refrigerant and also to overcome the frictional loss and pressure drop across the pipe we need some pumping power. There are varieties of compressors like; reciprocating compressors, rotary screw compressors, centrifugal compressors, scroll compressors and hermetically sealed compressor which are commonly used in refrigeration systems depending upon the requirements.

In this setup hermetically sealed compressor for 165L capacity has been used. Normally in hermetic and mainly semi-hermetic compressors the compressor and motor driving the compressor are integrated, and run inside the refrigerant system. The motor is hermetic and is intended to operate, and be cooled by the refrigerant being compressed.

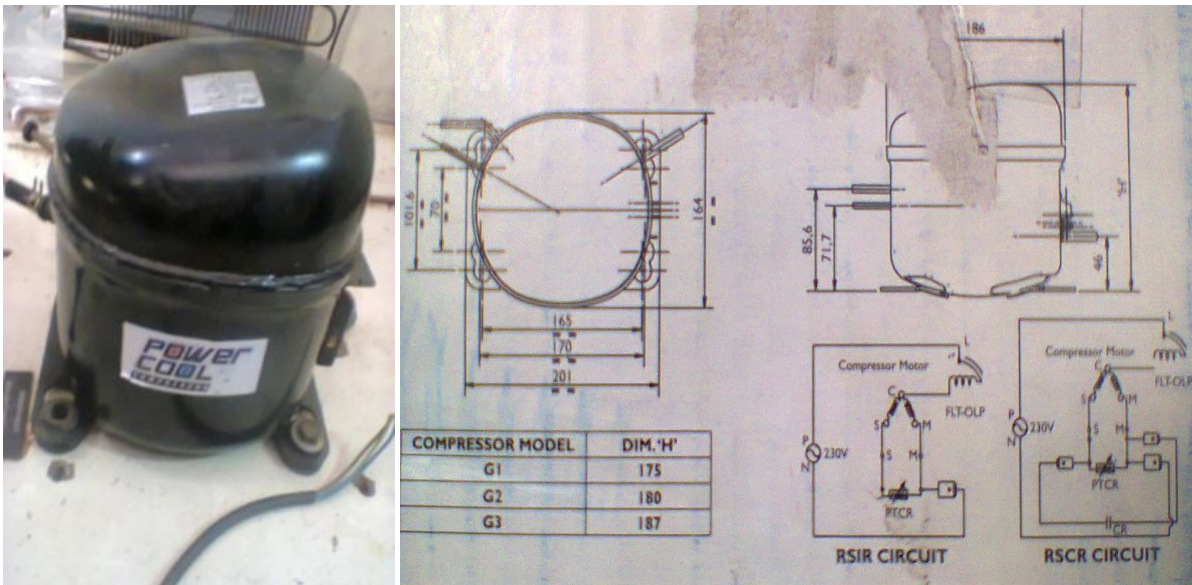


Fig.5.4: Compressor, dimension and circuit diagram

Compressor specifications		
Manufacturer	Godrej & Boyce Mfg. Co. Ltd.	
Model	Power cool comp R134a G1-1+CAPCT	
Dimensions	m*m*m	0.201*0.164*0.175
Capacity	Btu/hr.	410
Motor input	Watts	107
EER	Btu/Whr.	3.83
Displacement	CC	4.6
Voltage range	V	150-260
L.V. Pickup	V	160V
Oil charge	CC	300
Net weight	Kg	7.8
Overload protector		OLPA

Table 5.2: Compressor specifications

5.7.2 Refrigerant Flow Control Device

An expansion valve is a component in vapour compression refrigeration system that controls the quantity of refrigerant flow into the evaporator. It has two jobs to perform, it allows liquid refrigerant to enter the evaporator with desired pressure and at the same time maintains the required pressure & temperature in the evaporator. There are varieties of expansion devices as listed below which are commonly used.

- (i) Capillary tube
- (ii) Automatic expansion valve
- (iii) Thermostatic expansion valve

In this setup to control the flow in the system hand operated expansion valve has been used. The valve needle remains open during steady state operation. The size of the opening or the position

of the needle is related to the pressure and temperature of the evaporator. Smaller is the opening lower is pressure and temperature after expansion device.



Fig.5.5: Hand operated expansion valve

5.7.3 Condenser

A condenser is a device used to condense a substance from its gaseous to its liquid state. In vapour compression refrigeration system condenser is used to condense vapor refrigerant into liquid phase. It is the part of the system which rejects heat to the environment. Outlet of the compressor is connected to the inlet of condenser. It rejects the heat to the environment through the surface which is either air cooled or water cooled. The heat rejection capacity of a condenser is influenced by these factors:

- (i) The temperature difference between the refrigerant and the cooling media
- (ii) The flow rate of the cooling media through the condenser
- (iii) The flow rate of the refrigerant through the condenser

Types of condensers:

- (i) Finned-static condenser

(ii) Finned-forced convection condenser

(iii) Wire-static condenser

(iv) Plate-static condenser

In this setup natural draft Finned-static condenser has been used.



Fig.5.6: Finned static condenser

Condenser specifications	
Type	Natural draught
Diameter of pipe	0.00635 m
Length of pipe	13.7 m
Area of condenser	0.2732 m ²
Material	Copper

Table 5.3: Condenser Specifications

5.7.4 Evaporator

The liquid refrigerant entering the evaporator from the refrigerant flow control device is suddenly under low pressure there by its temperature decreases. Evaporator makes contact with the water and the medium from which heat has to be removed. Here liquid refrigerant changes phase.

In this set up emersion coil type evaporator is used. Evaporator is dipped in 10.5 litre of water.

Water is regularly circulated with agitator to ensure uniform heat transfer.

The rate of heat exchange with in an evaporator is governed by these factors:

- (i) The temperature difference between the refrigerant and the water being cooled
- (ii) The flow rate of the water through the evaporator
- (iii) The flow rate of the refrigerant through the evaporator

Types of Evaporator:

- (i) Plate type evaporator
- (ii) Bare type evaporator
- (iii) Forced convection evaporators
- (iv) Dry expansion evaporators
- (v) Flooded evaporators
- (vi) Shell and coil evaporators
- (vii) Shell and tube evaporators

Evaporator specifications	
Type	Emersion coil type
Dia. of pipe	0.00635 m
Length of pipe	7.62 m
Area of condenser	0.152 m ²
Material	Copper

Table 5.4: Evaporator specifications

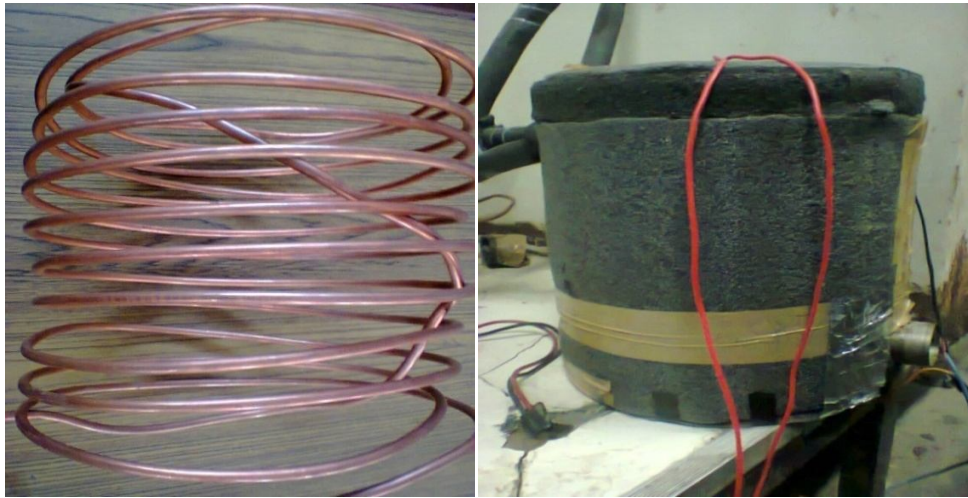


Fig.5.7: Coil type evaporator

5.7.5 Filter: There are number of components which can be damaged by the impurities present in the vapour compression refrigeration system. Compressor, expansion device can damage due to the impurities. To obstruct any impurity present in the system and to avoid any kind of choking filter has been used in experimental setup at condenser outlet. Mesh size of filter varies from (5-5000) micrometers. Nanoparticles can pass through this filter easily.



Fig 5.8: Filter

5.7.6 Heating element: An heating element convert electricity into heat through the procedure of resistive or Joule heating. Refrigerant takes the heat from the water present in evaporator and heating element adds heat to the evaporator at constant rate. It is used to give heating load or to maintain the required flux or temperature in the evaporator. In this setup metal heating element is used.



Fig.5.9: Heating element

Heater	
Specification	230V,50Hz A/C
Power	230W

Table 5.5: Heater

5.7.7 Pressure gauges: To measure pressure of the R134a Refrigerant at respective points. Four pressure gauges are used. One gauge is at compressor outlet, and other at condenser outlet, one gauge after expansion device and other after evaporator outlet. Commonly bourdon tube type refrigeration pressure gauges are used to measure the pressure. The bourdon pressure gauge uses the principle that a flattened tube tends to straighten or regain its original form in cross-section when pressurized. A vacuum gauge is used to measure the pressure in a vacuum. In this set up two types of gauges are used high pressure gauge and low pressure gauge.

Pressure gauge specifications	
High pressure side	0-300 psi
Low pressure side	(-30) - 150 psi

Table 5.6: Pressure gauge specifications



Fig.5.10: Pressure gauge

5.7.8 Rotameter: A rotameter consists of tube, normally made of glass with a float, actually a shaped weight, inside that is pushed up by the drag force of the flow and pulled down by gravity. To see the flow rate of refrigerant glass tube rotameter has been used. The position of rotameter is vertical. The rotameter range is 4-40LPH. The liquid refrigerant coming from the condenser passes through the rotameter and in this way moving element gives reading. The rotameter is manufactured by Zest engineering Delhi.



Fig.5.11: Glass tube type rotameter

5.7.9 Refrigerant: Refrigerant plays a great role in the vapour compression refrigeration system. Its thermodynamic properties decide the components design. In this experimental setup R134a refrigerant has been used. R134a is a halo-alkanes refrigerant with thermodynamic properties similar to refrigerant R12 but with a smaller amount of ozone depletion potential.



Fig.5.12: Refrigerant

Refrigerant properties	
Manufacturer	Seattle Gas, Italy
Purity	0.999
Moisture	5ppm(max)
Acidity	0.1ppm(max)
Vapour residue	100ppm (max)
Product	1.1.1.2-Tetraflouroethane

Table 5.7: Refrigerant properties

5.7.10 Voltmeter: A voltmeter is a device used to calculate electrical potential difference between two points in an electric circuit. Analog voltmeters move a pointer across a scale in proportion to the voltage of the circuit. The instrument is designed such that it disturbs the

circuit as little as possible so the instrument should draw a smallest amount of current to operate. This is achieved by using a sensitive galvanometer in series with a high resistance.

There are two types of voltmeters:

- (i) Analog voltmeter
- (ii) Digital voltmeter



Fig.5.13: Voltmeter

Voltmeter	
Manufacturer	ESS VEE Electricals
Type	72 mm ²
Range	0-300 V

Table 5.8: Voltmeter

5.7.11 Ammeter: An ammeter is a measuring device used to calculate the electric current in an electrical circuit. The bulk of ammeters are also connected in series with the circuit carrying the electrical current to be measured. Electric currents are measured in amperes (A). In this set up digital ammeter has been used.

Types of ammeters:

- (i) Moving-coil
- (ii) Moving magnet
- (iii) Electrodynamic
- (iv) Digital
- (v) Integrating



Fig.5.14: Ammeter

Ampere meter	
Manufacturer	Pyrotron
Type	Digital
Range	0-15 amp.

Table 5.9: Ampere meter

5.7.12 Energy meter: An Energy meter is an instrument that measures the amount of electric energy consumed by an electrically powered machine. It measures power input to the system. There are two energy meters used in the system. One is used to measure the power consumed by the compressor and other to measure the power consumed by the heater. The unit of energy is kilowatt hour (kWh). The energy input for both the devices is used to calculate the coefficient of performance of the system.

Types of energy meter:

- i) Electromechanical meters
- ii) Electronic meters
- iii) Solid-state design



Fig.5.15: Energy meter

Energy meter	
Manufacturer	Jaipur Metals and Electricals
Type	AC, 1 Phase, 2 wire, 50Hz
Range	0-20 amp
Rev/kWh	600

Table 5.10: Energy meter

5.7.13 Digital temperature controller: Temperature control is a process in which variation of temperature of a space is measured and the passage of heat energy into or out of the space is adjusted to achieve a desired temperature. Digital temperature controller is used to cut off the heater supply when the temperature exceeds a particular value in the evaporator. It is connected to a Relay device which is connected to heating element. This device sends signal to the relay

switch which cuts off the supply as well as on the supply of the heating element. There is a sensing element which always dipped in the evaporator water. With the help of digital temperature controller constant heat flux in the evaporator can be maintained.



Fig.5.16: Digital temperature controller

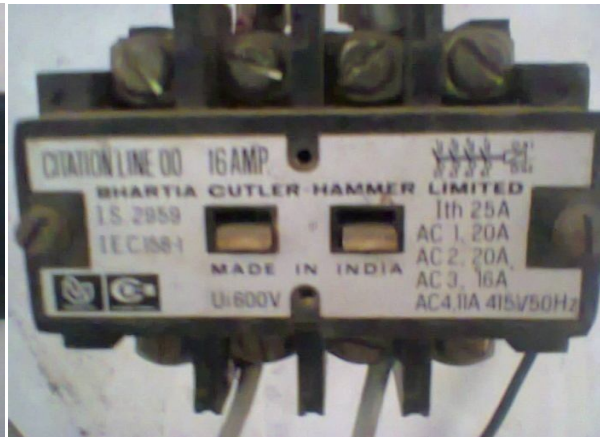


Fig.5.17: Relay switch

Digital temperature controller	
Manufacturer	ACR Inst & Valve Pvt. Ltd.
Type	Digital
Range	(-40)°C – 50°C

Table 5.11: Digital temperature controller

5.7.14 Hand shut off valve: A valve is a device that regulates, directs or controls the flow of a fluid by opening, closing, or partially obstructing various passageways. Hand shut off valves are used to close the flow in the line. It is also used to divert the flow towards rotameter. Four valves of this type are used. One valve is fitted at charging line inlet. Two valves are used at each end of rotameter. If there is need to by pass the flow then valve which is present parallel to the rotameter is opened.



Fig.5.18: Hand shut off valve

5.7.15 Temperature gauge (Mercury glass thermometers): Mercury glass thermometer consists of a bulb containing mercury attached to a glass tube of fine diameter. The volume of mercury in the tube is very small than the volume in the bulb. With the increase in temperature the volume of mercury changes slightly. This change in volume of mercury drives the mercury column a fairly long way up the tube. The space above the mercury may be filled with nitrogen or under partial vacuum. To measure the temperature at all points of the vapour compression refrigeration system we need mercury thermometers. These are used at compressor outlet, condenser outlet, after expansion valve and at evaporator outlet. With this temperature drop in condenser and temperature gain evaporator can be measured. Also to measure the ambient condition mercury glass thermometer is used.



Fig.5.19: Mercury glass thermometers

5.7.16 Flexible charging line: A flexible hose is used to transfer gas from the refrigerant cylinder to the compressor charging line. Line is connected to the gas cylinder and then connected to the $\frac{1}{4}$ inch valve from where refrigerant goes in the vapour compression system.



Fig.5.20: Flexible charging line

5.7.17 Vacuum pump: Vacuum pump is a compressor similar to the compressor used in the vapour compression refrigeration system. After completion of setup it has to be checked for any leakage. This is done by charging the system with the air. Also before charging refrigerant the vacuum is produced in the system to remove moisture or any air.



Fig.5.21: Vacuum pump

5.8 Vapour compression refrigeration tools and materials

5.8.1 Tubing

Most tubing used in refrigeration and air conditioning is made of copper.



Fig.5.22: Copper Tubing

Soft copper tubing is used in some commercial refrigeration and air conditioning work. It is annealed. This makes it flexible, therefore easy to bend and flare. These tubes are sold in rolls of 25+, 50+, 100 feet long.

5.8.2 Connecting tubing

1) Flared connections: Flare fittings are a category of compression fitting used with metal tubing, mostly ductile copper. A flare nut is used to secure the flared tubing's tapered end making a leak-tight seal. The tool consists of a die that grips the tube and a mandrel that is forced into the end of the tube to form the flare by cold working. The most ordinary flare fitting used is the 45-degree SAE style. Flared fittings are alternatives to solder-type joints when the use of an open flame is not preferred. To connect a valve to the pipe flared connections are used.



Fig.5.23: Flared connections



Fig.5.24: Flared type fittings



Fig.5.25: Flare nut ¼ inches

2) Soldered or brazed fitting

Soldered joints are used for water pipes and drains. Silver brazed joints are used for refrigerant pipe and tubing. Brazing is a metal joining process in this a filler metal is heated above melting point and spread between two or more close fitting parts by capillary action. In experimental setup for joining of pipes and pressure gauges brazing is used.

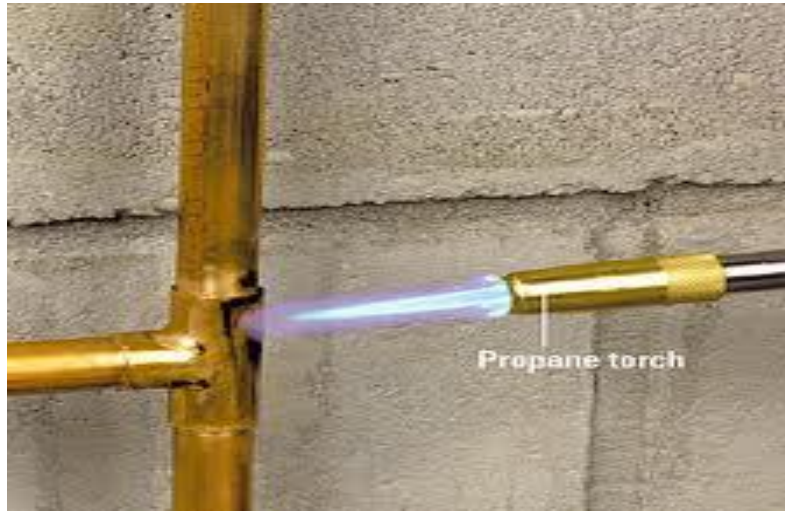


Fig.5.26: Brazed tubing

5.8.3 Hand tools used: For preparation of the experimental setup numbers of hand tools are used.

These are listed below.

Wrenches	Machine screws	Cap screws	Gaskets
Vises	Hammers	Pliers	Service valves
Mandrel	Twist drills	Dies	Stamps
Abrasives	Hack saw	Measuring rules and tapes	Instruments and gauges
Files	Brushes	Tube cutter	Micrometer
Bolts	Hacksaws	Fastening devices	Cold chisels
Brazing torch	Adjustable wrench	Allen wrench	Nut drivers
Open wrench	Electric drill Gun	Swaging tool	Copper tube bender

Table 5.12: Hand tools used

RESULTS AND DISCUSSION

After conducting experiments with pure R134a refrigerant, refrigerant R134a + 0.25% SiO₂, refrigerant R134a + 0.40% SiO₂, refrigerant R134a + 0.25% Al₂O₃ and with refrigerant R134a + 0.40% Al₂O₃ readings have been taken for pressure, temperature, energy at 11 LPH volume flow rate for two types of fluxes and for cooling load temperature-time analysis. Graphs are drawn for coefficient of performance (COP) of refrigeration system, temperature drop in condenser and temperature gain in evaporator. All the parameters are summarized in tables below.

Refrigerant	Evaporator temperature load at (25-26 °C)									
	COP	P1 (kg/cm ²)	P2 (kg/cm ²)	P3 (kg/cm ²)	P4 (kg/cm ²)	T1 (°C)	T2 (°C)	T3 (°C)	T4 (°C)	Tatm (°C)
R134a	0.68	214.077	212.828	22.538	18	84.35	51.46	0.63	26	33.54
R134a+SiO ₂ (0.25gm)	0.69	216.923	215.231	22.538	16.92	85.54	50.85	-2.12	25	31.96
R134a+SiO ₂ (0.4gm)	0.75	219.077	217.077	21.077	16.87	85.52	51.04	-2.06	25.37	32.42
R134a+Al ₂ O ₃ (0.25gm)	0.68	218.154	216.988	20.662	17.25	84.73	47.77	-1.5	25.27	32.27
R134a+Al ₂ O ₃ (0.4gm)	0.74	211.692	209.538	20.307	17.5	84.65	48.12	-2.04	25.35	33

Table 6.1: COP, pressure and temperature for R134a refrigerant and nanorefrigerants at 11 LPH volume flow rate and heat flux at 25-26 °C

Refrigerant	Evaporator temperature load at (35-36 °C)									
	COP	P1 (kg/cm ²)	P2 (kg/cm ²)	P3 (kg/cm ²)	P4 (kg/cm ²)	T1 (°C)	T2 (°C)	T3 (°C)	T4 (°C)	Tatm. (°C)
R134a	0.87	216.923	215.077	23.461	18.57	86.27	52.19	1.04	33.19	33.40
R134a+SiO ₂ (0.25gm)	0.90	211.62	209.538	22.307	17.15	84.08	49.42	-1.58	32.69	29.77
R134a+SiO ₂ (0.4gm)	0.92	215.31	213.00	23.385	17.69	84.46	50.15	-1.73	32.55	29.73
R134a+Al ₂ O ₃ (0.25gm)	0.87	212.31	211.08	21.230	17.65	82.23	46.31	-1.35	33.23	30.27
R134a+Al ₂ O ₃ (0.4gm)	0.93	210.08	207.54	21.308	18.00	84.19	46.73	-1.46	33.00	31.04

Table 6.2: COP, pressure and temperature for R134a refrigerant and nanorefrigerants at 11 LPH volume flow rate and heat flux at 35-36 °C

6.1 Temperature drop in Condenser

The condenser consists of coils of pipe in which refrigerant at high pressure and temperature vapour refrigerant is cooled and condensed at constant pressure. Temperature drop in condenser is the difference of compressor outlet refrigerant temperature and condenser outlet refrigerant temperature. Higher the temperature drop in the condenser more is the heat rejected to the environment more is the refrigeration effect. The heat is first transferred to walls of the condenser tubes and then from tubes to cooling medium. In this experimental test rig air is used as cooling medium with natural convection and wire and tube type condenser is used. Sometimes, after condensation process refrigerant is cooled below saturation temperature before expansion. Such process is called subcooling of the refrigerant. The ultimate effect of subcooling is to increase the value of coefficient of performance. In following study temperature drop for refrigerant across the condenser has been studied.

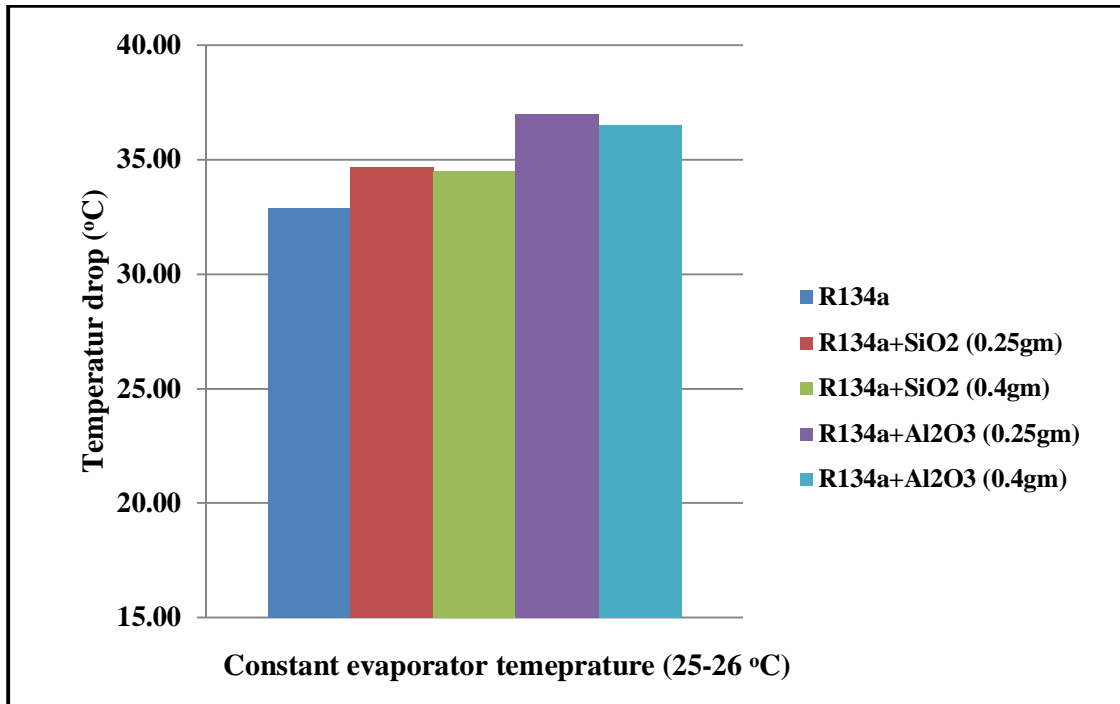


Fig.6.1: Temperature drop in condenser for nanorefrigerants at 11 LPH volume flow rate and heat flux at 25-26 °C

Fig.6.1 shows a temperature drop in condenser for 11 LPH volume flow rate of nanorefrigerant when constant evaporator heat load is applied at 25-26 °C and at ambient temperature of 32°C ± 2°C. For refrigerant R134a temperature reduction in condenser is 32.89°C, whereas with refrigerant R134a + 0.25% SiO₂ and R134a + 0.40% SiO₂ temperature drop is 34.69°C and 34.48°C respectively. So, a 5.47% more temperature drop with refrigerant R134a + 0.25% SiO₂ and a 4.83% more temperature drop with refrigerant R134a + 0.40% SiO₂, has been observed compared to temperature drop in case of pure refrigerant R134a. Also, with refrigerant R134a + 0.25% Al₂O₃ and R134a + 0.40% Al₂O₃ temperature drop of 36.96°C and 36.53°C is observed. So, It can be concluded that a 12.37% more temperature drop with refrigerant R134a + 0.25% Al₂O₃ and 11.06% improvement in temperature drop with refrigerant R134a + 0.40% Al₂O₃ is found compared to temperature drop for pure refrigerant R134a.

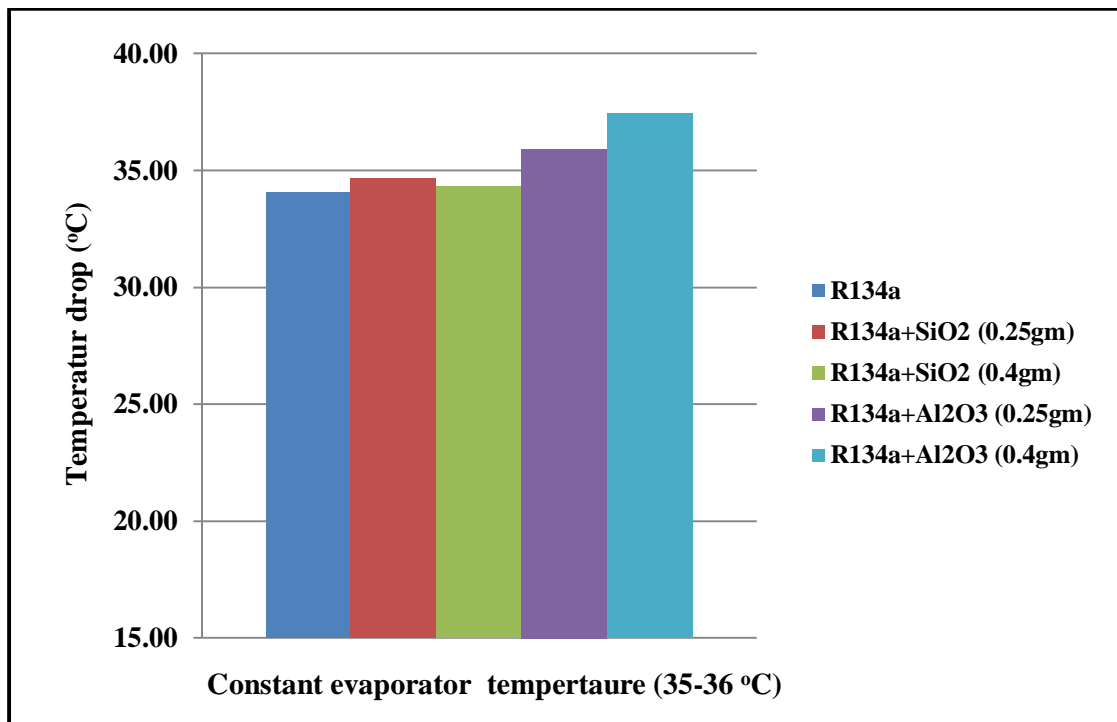


Fig.6.2: Temperature drop in condenser for nanorefrigerants at 11 LPH volume flow rate and heat flux at 35-36 °C

Same trend has been observed with 35-36 °C evaporator heat load and at ambient temperature of 31.5°C ± 2°C. For refrigerant R134a temperature reduction in condenser temperature is 34.08°C, whereas with refrigerant R134a + 0.25% SiO₂ and R134a + 0.40% SiO₂ drop is 34.66°C and 34.31°C respectively. Fig. 6.2 Shows a 1.7% more temperature drop with refrigerant R134a + 0.25% SiO₂ and a 0.67% increase in temperature drop with refrigerant R134a + 0.40% SiO₂ compared to temperature drop in case of refrigerant R134a. In case of refrigerant R134a + 0.0.25% Al₂O₃ and R134a + 0.40% Al₂O₃ temperature drop is found to be 35.92°C and 37.46°C respectively. So, It can be concluded that there is a 5.4% more temperatures drop with refrigerant R134a + 0.25% Al₂O₃ and 9.92% more temperature drop with refrigerant R134a + 0.4% Al₂O₃ compared to temperature drop in case of pure refrigerant R134a.

So results show that there is more temperature drop in condenser or in other words this drop in temperature aids subcooling to the refrigeration system which enhances the refrigeration in the system i.e. improved heat rejection in the condenser is achieved with nanorefrigerant. This subcooling is due to improvement in heat transfer characteristics of the nanorefrigerant. Investigation of Al_2O_3 based refrigerant shows more heat transfer as compared to SiO_2 based refrigerant at all concentrations. This is due to higher thermal conductivity of Al_2O_3 based refrigerant as compared to SiO_2 based refrigerant. So, overall it is concluded that the effects of above mentioned nanorefrigerant is to increase the heat rejection in the condenser of the refrigeration system.

6.2 Temperature gain in Evaporator

After expansion, liquid-vapour mixture of refrigerant at low pressure and temperature enters into the evaporator, where it evaporates at constant pressure and temperature. During evaporation process refrigerant absorbs its latent heat of vaporization from the medium to be cooled as water in this experiment. Temperature gain in evaporator is the difference of evaporator outlet temperature and evaporator inlet temperature. Higher is the gain in the evaporator temperature higher is the heat carried by the refrigerant hence better is the performance of evaporator.

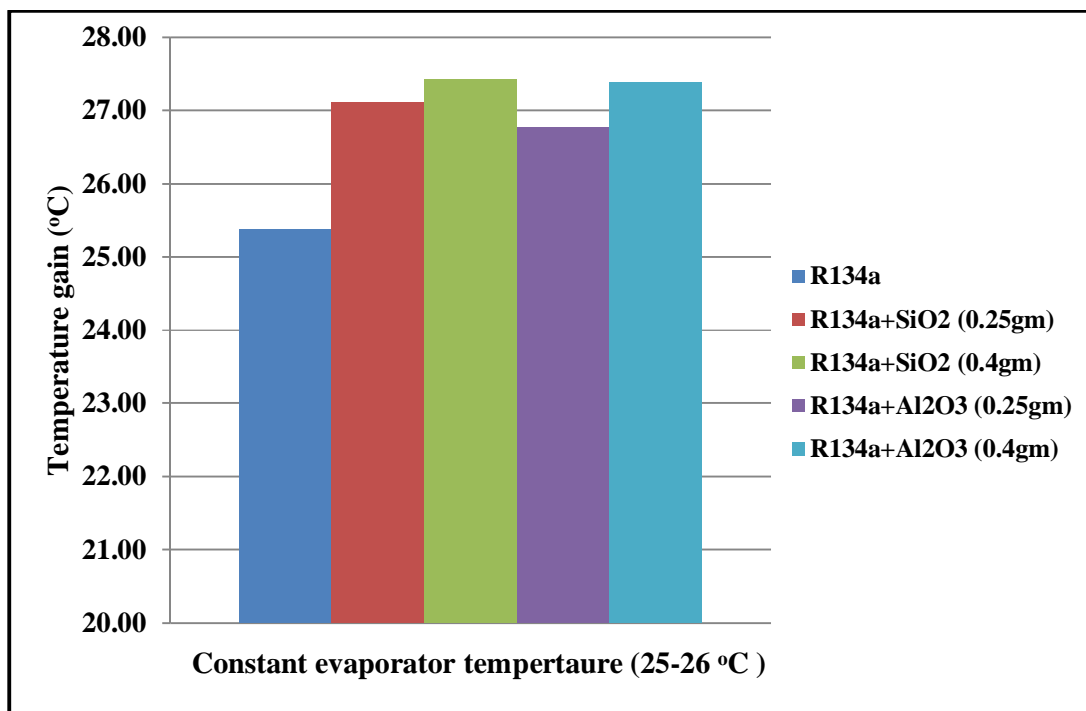


Fig.6.3: Temperature gain in evaporator for nanorefrigerants at 11 LPH volume flow rate and heat flux at 25-26 °C

Fig.6.3 shows temperature gain in evaporator for 11 LPH volume flow rate of the refrigerant where evaporator is maintained at constant heat load at 25-26 °C & at ambient temperature of 32°C ±2°C. For refrigerant R134a temperature gain in evaporator is 25.37°C, whereas with refrigerant R134a + 0.25% SiO₂ and R134a + 0.40% SiO₂ the temperature gain is 27.12°C and 27.42°C respectively. So a 6.89% more gain in temperature with refrigerant R134a + 0.25% SiO₂ and 8.08% more gain in temperature with refrigerant R134a + 0.40% SiO₂ has been observed compared to temperature gain for a pure refrigerant R134a. For refrigerant R134a + 0.025% Al₂O₃ and R134a + 0.40% Al₂O₃ gain in temperature is 26.77°C and 27.38°C respectively. So a 5.51% more temperature gain in evaporator with refrigerant R134a +0.25% Al₂O₃ and a 7.92% more temperature gain with refrigerant R134a +0.4% Al₂O₃ is achieved as compared to temperature gain for refrigerant R134a.

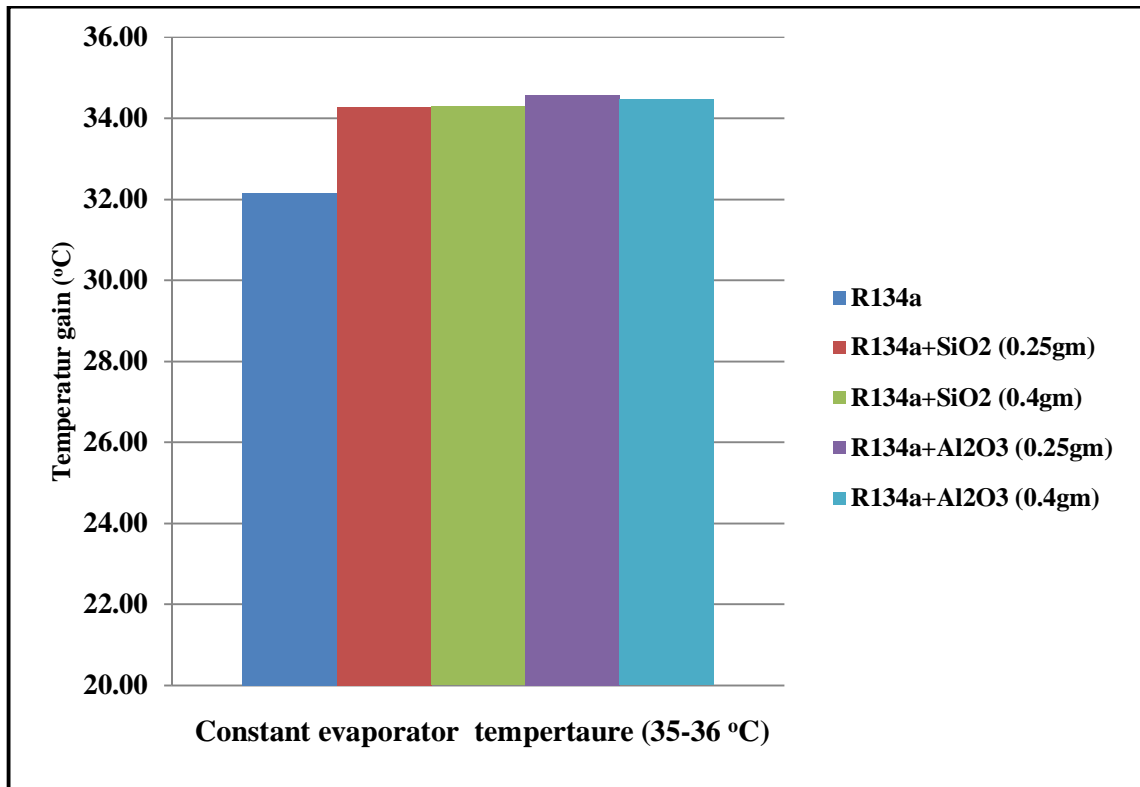


Fig.6.4: Temperature gain in evaporator for nanorefrigerants at 11 LPH volume flow rate and heat flux at 35-36 °C

Same trend has been observed when evaporator heat flux is maintained at 35-36 °C and ambient temperature at 31.5°C ±2°C. Here in Fig.6.4, for refrigerant R134a temperature gain in evaporator is 32.15°C, whereas with refrigerant R134a + 0.25% SiO₂ and R134a + 0.40% SiO₂ gain in temperature in evaporator is 34.27°C and 34.28°C respectively. So a 6.59% more temperature gain with refrigerant R134a + 0.25% SiO₂ and 6.62% enhancement in temperature gain with refrigerant R134a + 0.40% SiO₂ have been observed as compared to refrigerant R134a. With refrigerant R134a + 0.25% Al₂O₃ and R134a + 0.40% Al₂O₃ gain in temperature is 34.58°C and 34.46°C respectively. So a 7.55% more temperature gain with refrigerant R134a + 0.25% Al₂O₃ and 7.18% more temperature gain with refrigerant R134a + 0.40% Al₂O₃ is achieved compared to temperature gain for refrigerant R134a.

So from above we can justify that mixing of nanoparticles with refrigerant results an improvement in the heat transfer characteristics of evaporator. It improves the heat transfer coefficient.

6.3 Coefficient of performance (COP)

COP is defined as the ratio of refrigeration effect and work input to the system. In this case COP is the ratio of power input to heater submerged in evaporator water to the power consumed by the compressor.

$$\text{COP} = \frac{\text{Refrigeration Effect}}{\text{Work Done}}$$

COP is highly influenced by operating conditions, especially ambient temperature and relative temperatures between sink and system. Here in this experimental study actual COP of refrigeration system has been investigated.

In present study, coefficient of performance for the system and effect of nanorefrigerant on it has been investigated. Similarly, readings are taken for pure refrigerant R134a, refrigerant R134a + 0.25% SiO₂, refrigerant R134a + 0.40% SiO₂, refrigerant R134a + 0.25% Al₂O₃ and refrigerant R134a + 0.40 % Al₂O₃. First study is performed at 11 LPH volume flow rate of the refrigerant and at constant evaporator heat load at 25-26 °C, when ambient temperature is around 33°C ±1°C.

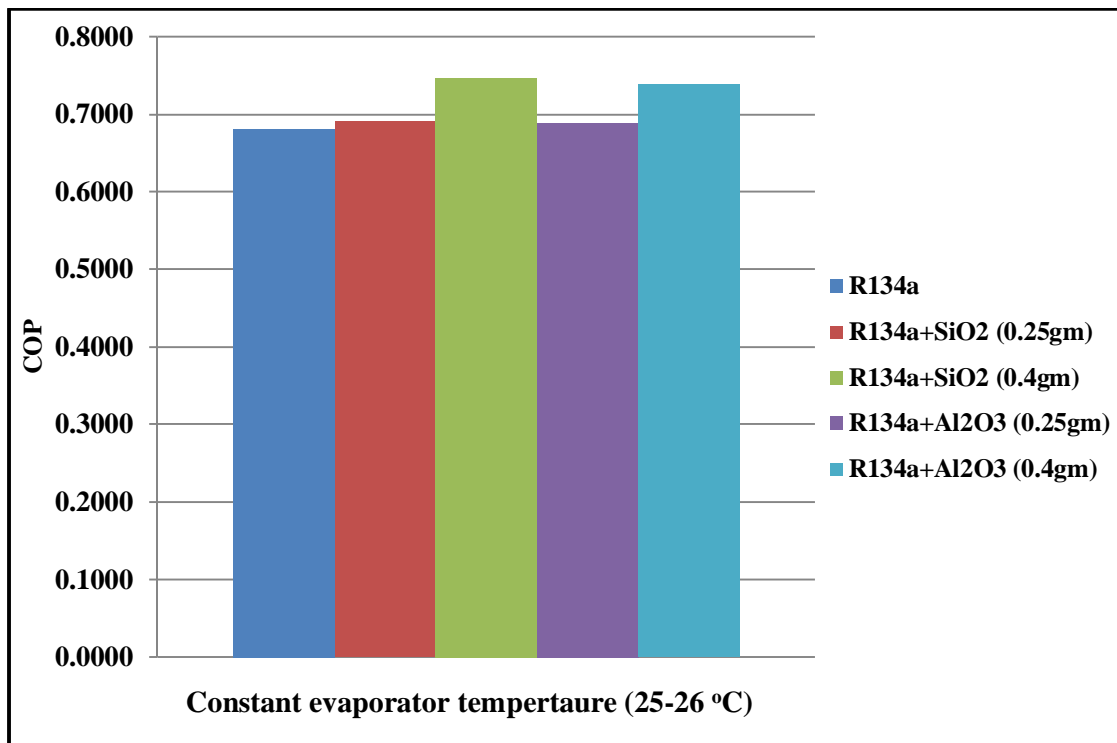


Fig.6.5: COP comparison for nanorefrigerants at 11 LPH volume flow rate and heat flux at 25-26 °C

As shown in Fig. 6.5, COP with pure refrigerant R134a is found to be 0.68 and with nanorefrigerant R134a + 0.25% SiO₂ and refrigerant R134a + 0.40% SiO₂, COP is 0.69 and 0.74 respectively. With nanorefrigerant R134a + 0.25% Al₂O₃ and refrigerant R134a + 0.40% Al₂O₃, COP is 0.68 and 0.73 respectively. So there is a 1.41% and 9.72% improvement in COP for refrigerant R134a + 0.25% SiO₂ and refrigerant R134a + 0.40% SiO₂ and with refrigerant R134a + 0.25% Al₂O₃ and refrigerant R134a + 0.40% Al₂O₃ improvement in performance is 1.175% and 8.40% as compared to refrigerant R134a.

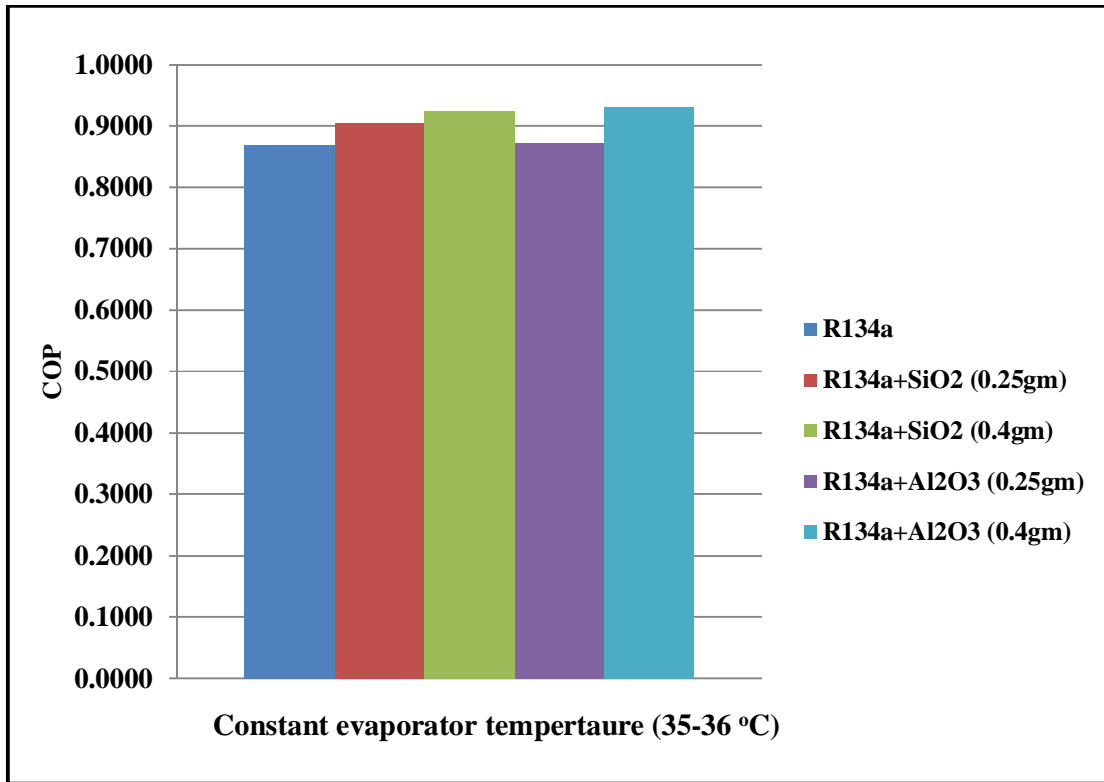


Fig.6.6: COP comparison for nanorefrigerants at 11 LPH volume flow rate and heat flux at 35-36 °C

Same study has been performed at 11 LPH volume flow rate and 35-36 °C evaporator temperature and at 31.5°C ±2°C ambient temperature. As shown in Fig.6.6, COP for pure refrigerant R134a is 0.86 and with nanorefrigerant having R134a + 0.25% SiO₂ and R134a + 0.40% SiO₂, COP is 0.90 and 0.92 respectively. With nanorefrigerant R134a + 0.25% Al₂O₃ and R134a + 0.40% Al₂O₃, COP is 0.87 and 0.93 respectively. So it has been concluded that there is a 4.05% and 6.23% improvement in performance for refrigerant R134a + 0.25% SiO₂ and refrigerant R134a + 0.40% SiO₂. With refrigerant R134a + 0.25% Al₂O₃ and refrigerant R134a + 0.40% Al₂O₃ improvement in performance is 0.32% and 6.88%. Hence there is increase in the COP of the system with addition of nanoparticles in the refrigerant and also with increases in mass fraction of nanoparticles.

6.4 Temperature-time graph: An experiment study is conducted to estimate cooling capacity of refrigeration system. First heat is given to water present in the container around the evaporator coil. The temperature has been raised to 40°C and then with the help of refrigeration system temperature is reduced to 25°C. A study has been performed to bring down temperature from 40°C to 25°C at 11 LPH volume flow rate for pure refrigerant R134a, refrigerant R134a + 0.25% SiO₂, refrigerant R134a + 0.40% SiO₂, refrigerant R134a + 0.25% Al₂O₃ and refrigerant R134a + 0.40% Al₂O₃. In these experiments evaporator temperature decreases until it reaches a desired value. During these, readings for power consumption, pressures, time taken and temperature at all respective points are noted. Readings and graphs are shown below.

Pure refrigerant R134a																
Flow rate (LPH)	11															
Temp. (°C)	40	39	38	37	36	35	34	33	32	31	30	29	28	27	26	25
Time taken (hh:mm)	0	0:05	0:11	0:16	0:21	0:27	0:32	0:37	0:44	0:50	0:55	1:03	1:11	1:16	1:24	1:33
P1 (kg/cm ²)	216	216	215	216	217	216	214	215	220	218	216	216	216	217	217	218
P2 (kg/cm ²)	214	215	214	215	216	215	213	215	220	216	215	215	215	216	215	216
P3 (kg/cm ²)	24	23	24	24	24	23	21	20	24	24	24	24	24	24	24	24
P4 (kg/cm ²)	19	18.5	19	18.5	19	18.5	18	16.5	19	19	18.5	19	19	19	19	19
T1 (°C)	87	87	87	87	87.5	87	86	86	86	86	87	86	85.5	85.5	86	86
T2(°C)	52.5	52.5	52.5	53	52.5	52.5	52	52	52.5	52	52	52	52	52.5	52.5	52
T3 (°C)	1	0.5	0.5	0.5	0.25	1	1	0	1	0.5	0	1	1	1	1	1
T4 (°C)	35.5	35	34.5	34	33.5	33.25	32	31	30	29	28	27.5	27	26	25.5	25
Tatm. (°C)	29.5	29.5	29.5	29.5	30	30	30	30	30	30	30	30	30	30	30.5	30.5
E comp.(kw)																0.23

Table 6.3: Temperature –time data for refrigerant R134a at 11 LPH volume flow rate

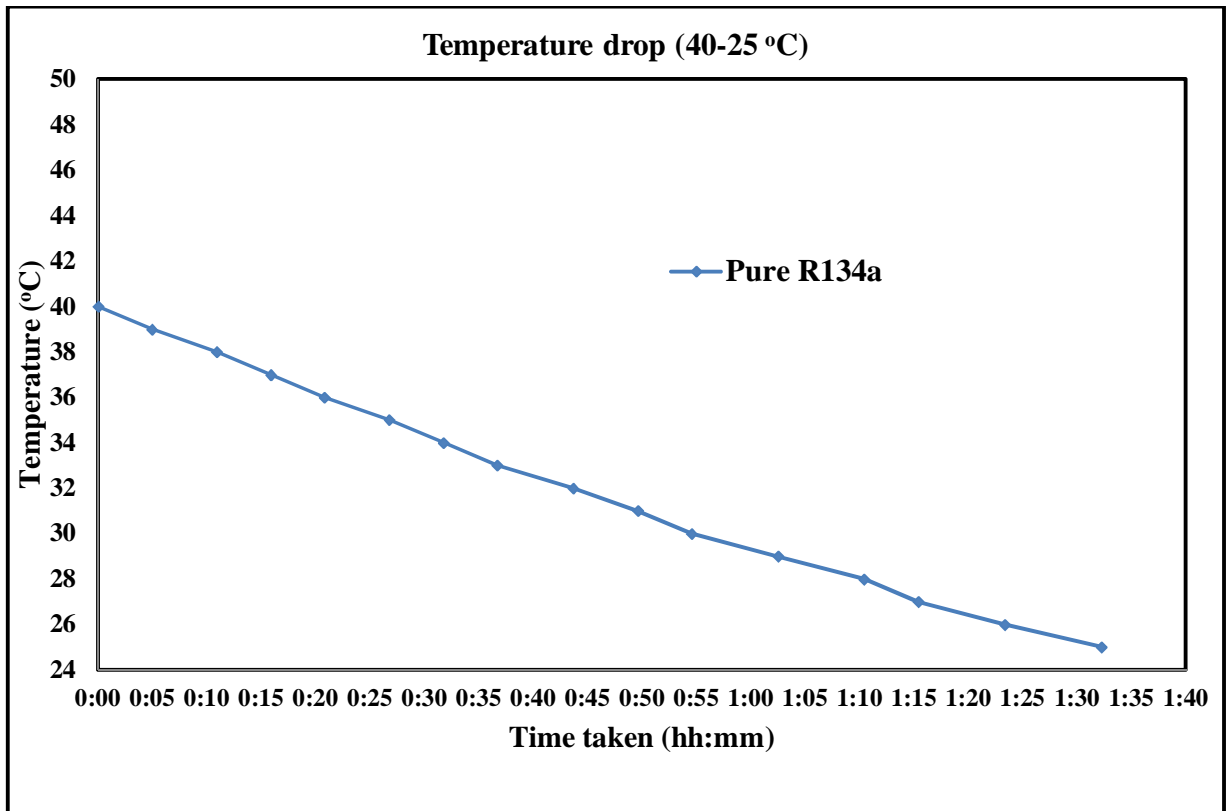


Fig.6.7: Temperature-time graph for R134a refrigerant at 11 LPH volume flow rate

Fig.6.7 represents the temperature - time analysis for 11 LPH volume flow rate at $30^{\circ}\text{C} \pm 1^{\circ}\text{C}$ ambient temperature. In this study it is found that pure refrigerant R134a takes 1 hour 33 minutes for temperature to come down from 40°C to 25°C .

R134a + SiO ₂ (0.25gm)																
Flow rate(LPH)	11															
Temp.(°C)	40	39	38	37	36	35	34	33	32	31	30	29	28	27	26	25
Time taken (hh:mm)	0	0:02	0:08	0:14	0:19	0:25	0:31	0:38	0:46	0:51	0:57	1:06	1:13	1:20	1:30	1:36
P1(kg/cm ²)	220	220	217	220	218	213	215	219	219	216	220	220	216	213	213	212
P2(kg/cm ²)	218	218	215	218	216	212	214	218	217	214	218	219	214	211	211	210
P3(kg/cm ²)	24	24	23	23	23	24	24	23	23	23	23	23	23	23	21	21
P4(kg/cm ²)	18.5	18	17	17.5	17.5	18	18	17.5	17	17	17	17	17.5	17	16.5	16.5
T1(°C)	88	87.5	87.5	88	87	86.5	87.5	87.5	87	86.5	87	87	86.5	86.5	86	86
T2(°C)	51	51	51	51	51	51	51	51	51	51	51	51	51	51	51	51
T3(°C)	-1	-1	-1	-1	-1	-1.5	-1.5	-1	-1.5	-2	-1.5	-1.5	-1.5	-1.5	-2	-2
T4(°C)	35	35	34.5	33.7	33	32.5	32	31	30	29	28	27.5	27	26.2	25.5	25
Tatm.(°C)	31	31	31	31	31	31	31	31	31	31	31	31	31	31.5	31.5	31.5
E comp. (kw)																0.205

Table 6.4: Temperature –time data for refrigerant R134a+ SiO₂ (0.25gm) at 11 LPH volume flow rate

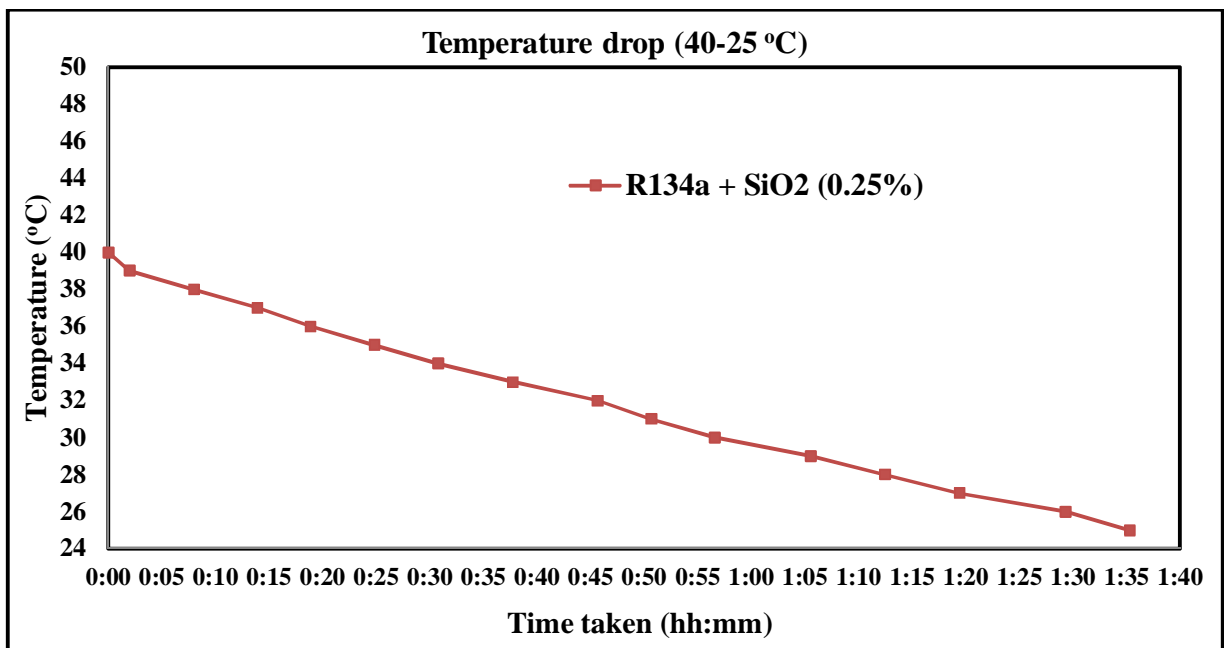


Fig.6.8: Temperature-time graph for refrigerant R134a+ SiO₂ (0.25gm) at 11 LPH volume flow rate

Fig.6.8 represents the cooling load temperature - time analysis for 11 LPH volume flow rate at $31^{\circ}\text{C} \pm 1^{\circ}\text{C}$ ambient temperature. In this study it is found that refrigerants R134a + 0.25% SiO₂ takes 1 hour 36 minutes.

R134a + SiO ₂ (0.4gm)																
Flow rate(LPH)	11															
Temp.(°C)	40	39	38	37	36	35	34	33	32	31	30	29	28	27	26	25
Time taken (hh:mm)	0	0:02	0:08	0:12	0:17	0:24	0:30	0:35	0:41	0:47	0:51	0:58	1:04	1:10	1:18	1:24
P1(kg/cm ²)	215	215	215	214	214	214	213	212	213	213	214	216	216	215	215	215
P2(kg/cm ²)	213	213	213	218	212	212	211	210	211	211	212	214	214	213	213	213
P3(kg/cm ²)	24	24	24	24	22	23	23	23	23	23	23	24	21	21	21	23
P4(kg/cm ²)	18	18	18	18	17	17.5	17.5	17.5	17	17	17	17.5	16.5	16.5	16.5	17.5
T1(°C)	87.5	87.5	86.5	86.5	87	87	86	87	85.5	85.5	85	85.5	85.5	84.5	84.5	84.5
T2(°C)	50.5	50.5	50.5	50	50	50	50	50	50	50	50	50	50	50	50	50
T3(°C)	-1.2	-1.2	-1.2	-1.2	-1	-1.2	-1.5	-1.5	-1	-1	-1.5	-1.2	-1	-1.5	-1.2	-1.5
T4(°C)	36	35.5	35	34	33	32	31	30.2	30	29.5	29	28.7	27.5	26	25	25
Tatm.(°C)	30.5	30.5	30.5	30.5	30.5	30.5	30.7	30.7	31	31	31	31	31	31	31	31
E comp. (kw)																0.2

Table 6.5: Temperature –time data for refrigerant R134a+ SiO₂ (0.40gm) at 11 LPH volume flow rate

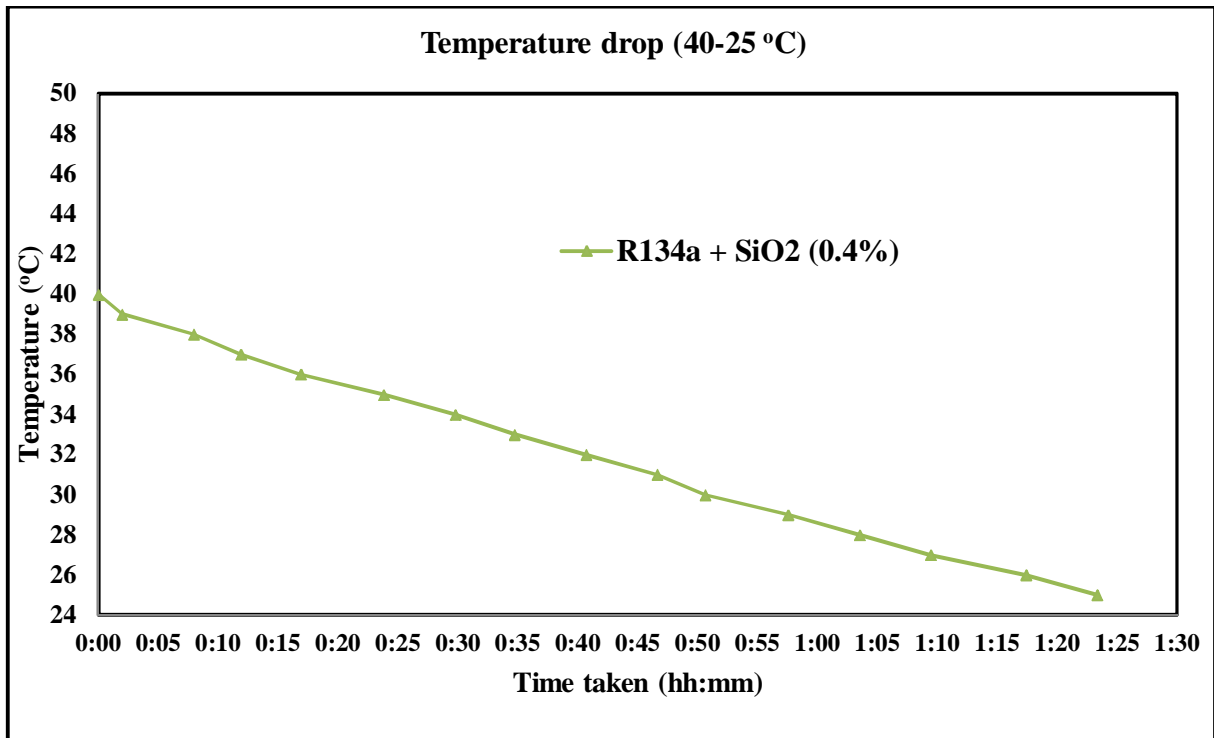


Fig.6.9: Temperature-time graph for refrigerant R134a+ SiO₂ (0.40gm) at 11 LPH volume flow rate

Fig.6.9 represents the cooling load temperature - time analysis for refrigerant R134a+ SiO₂ (0.40gm) at 11 LPH volume flow rate and at 30.5°C ±1°C ambient temperature. Refrigerant R134a + 0.40% SiO₂ takes 1 hour 24 minutes for temperature drop from 40°C to 25°C.

6.5 Cooling load temperature - time analysis for refrigerant R134a and SiO₂ based nanorefrigerants at 11 LPH volume flow rate

To know about the cooling capacity of the evaporator studies have been performed with pure refrigerant R134a, refrigerant R134a + 0.25% SiO₂ and refrigerant R134a + 0.40% SiO₂.

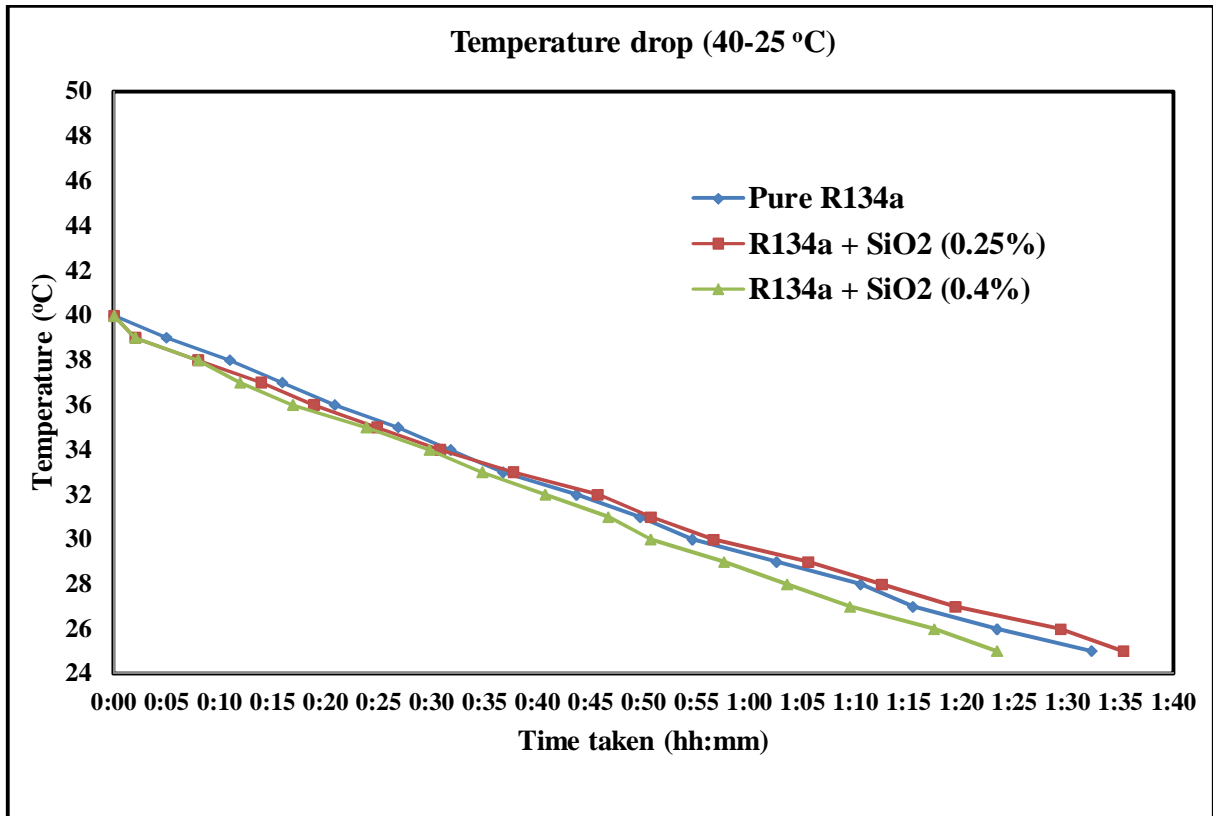


Fig.6.10: Temperature-time graph for refrigerant R134a and SiO₂ based nanorefrigerants at 11 LPH volume flow rate

Fig.6.10 represents the cooling load temperature - time analysis at 11 LPH volume flow rate and at ambient temperature of 30.5°C ±1°C. In this study it is observed that pure refrigerant R134a takes 1 hour 33 minutes for temperature drop from 40°C to 25°C, while nanorefrigerant R134a + 0.25% SiO₂ takes 1 hour 36 minutes. Refrigerant R134a + 0.40% SiO₂ takes 1 hour 24 minutes for temperature drop from 40°C to 25°C. So result shows a 3.23% increment in time for refrigerant R134a + 0.25% SiO₂ and 9.67% decreases in time to achieve temperature from 40°C to 25°C for refrigerant R134a + 0.40% SiO₂. It shows heat transfer is more effective with nanoparticles based refrigerants.

R134a + Al ₂ O ₃ (0.25gm)																
Flow rate (LPH)	11															
Temp.(°C)	40	39	38	37	36	35	34	33	32	31	30	29	28	27	26	25
Time taken (hh:mm)	0	0:04	0:10	0:16	0:20	0:25	0:30	0:36	0:44	0:49	0:55	1:03	1:09	1:15	1:24	1:30
P1(kg/cm ²)	216	216	218	215	217	218	220	220	216	216	216	216	216	217	218	216
P2(kg/cm ²)	215	215	216	214	215	215	219	219	215	215	215	215	216	216	216	215
P3(kg/cm ²)	22	22	23	21	21	21	21	21	22	21	22	22	21	21	21	21
P4(kg/cm ²)	19	19	19	18	18	18	18	18	18	17.5	18	18	18	18	17.5	18
T1(°C)	86	85.5	86	86	86	86.5	86.5	86	85.5	85	85	85	84.5	84.5	85	84.5
T2(°C)	47.5	47.5	47.5	47	47.5	47	47.5	47.5	47	47	47	47	47	47	47	47
T3(°C)	0	0	0	-0.5	-0.5	-0.5	-1	-1	-1.5	-1.5	-1	-1.5	-0.5	-1	-1	-1
T4(°C)	36	36	36	34.5	34	33	32	31	30	29	28.5	27.5	27	26.5	26	25
Tatm.(°C)	31	31	31	31	31	31	31	31	31	31	31	31.5	31.5	31.5	31.5	31.5
E comp.(kw)																0.22

Table 6.6: Temperature –time data for refrigerant R134a + Al₂O₃ (0.25gm) at 11 LPH volume flow rate

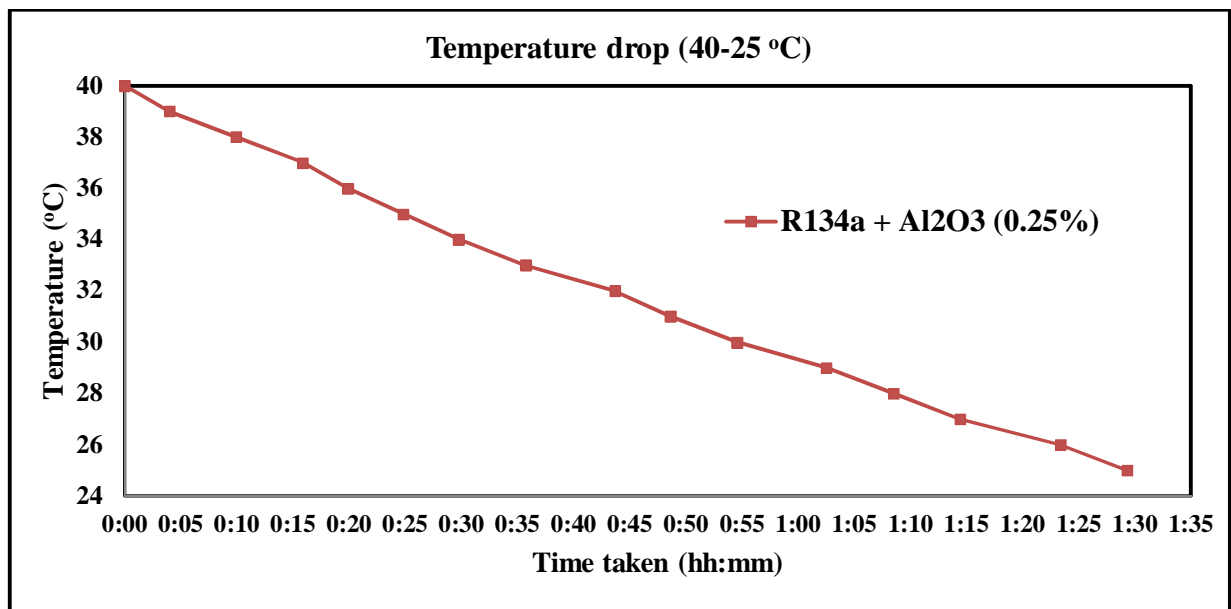


Fig.6.11: Temperature-time graph for refrigerant R134a+ Al₂O₃ (0.25gm) at 11 LPH volume flow rate

Fig.6.11 represents the cooling load temperature - time analysis for refrigerant R134a + Al₂O₃ (0.25gm) at 11 LPH volume flow rate and at 31°C ±1°C ambient temperature. Refrigerant R134a + Al₂O₃ (0.25gm) takes 1 hour 30 minutes for temperature drop from 40°C to 25°C.

R134a + Al ₂ O ₃ (0.40gm)																
Flow rate LPH	11															
Temp.(°C)	40	39	38	37	36	35	34	33	32	31	30	29	28	27	26	25
Time taken (hh:mm)	0	0:02	0:07	0:12	0:18	0:24	0:29	0:36	0:42	0:47	0:53	1:00	1:07	1:14	1:19	1:25
P1(kg/cm ²)	209	209	209	209	210	209	210	206	209	208	209	210	209	210	206	210
P2(kg/cm ²)	207	207	207	207	207	207	207	205	207	206	207	208	208	209	204	209
P3(kg/cm ²)	22	22	22	23	23	23	23	21	21	21	21	21	21	21	21	21
P4(kg/cm ²)	18	18	18	18	18	17.5	17	16	16	16	16	16	16	16	16	16
T1(°C)	86	86	86	86	86.5	85.5	85	85	84	84	84	83.5	83.5	83.5	83.5	83.5
T2(°C)	47	47	46.5	46.5	46.5	46.5	47.5	47.5	47.5	47.5	47.5	47	47	47.5	47.5	47.5
T3(°C)	-2	-2	-1	-1	-0.5	-0.5	-1	-1	-1	-1	-1	-1	-1.5	-1	-1.5	-1.5
T4(°C)	36.5	36.2	35.5	35	34	33	32	31	30.5	30	29.5	28.5	27.5	27	26	25.5
Tatm.(°C)	32	32	32	32	32.5	32.5	32.5	32.5	32.5	32.5	33	33	33	33	33	33
E comp.(kw)																0.2

Table 6.7: Temperature –time data for refrigerant R134a+Al₂O₃ (0.40gm) at 11 LPH volume flow rate

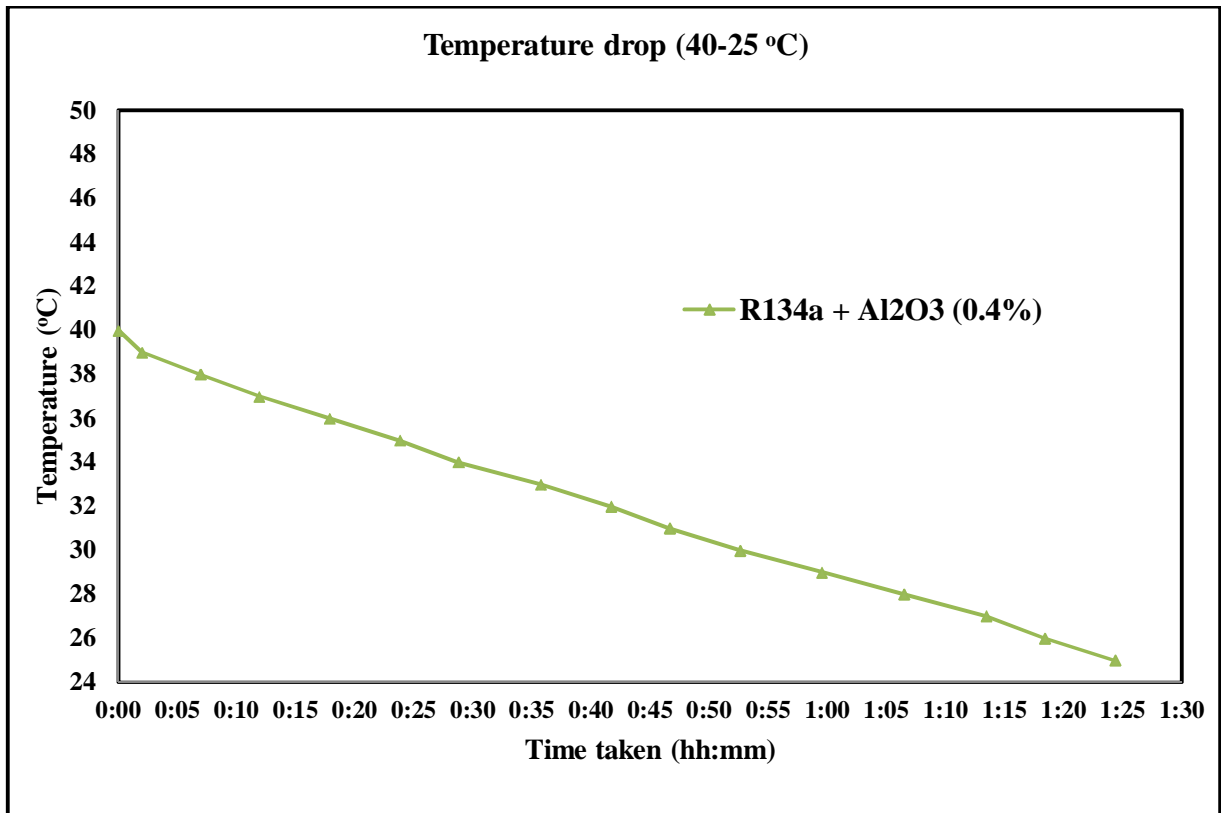


Fig.6.12: Temperature-time graph for refrigerant R134a + Al₂O₃ (0.40gm) at 11 LPH volume flow rate

Fig.6.12 represents the cooling load temperature - time analysis for refrigerant R134a +0.40 % Al₂O₃ at 11 LPH volume flow rate and at 32°C ±1°C ambient temperature. Refrigerant R134a +0.40 % Al₂O₃ takes 1 hour 25 minutes for temperature drop from 40°C to 25°C.

6.6 Cooling load temperature - time analysis for refrigerant R134a and Al₂O₃ based nanorefrigerants at 11 LPH volume flow rate

To know about the cooling capacity of the evaporator studies have been performed with pure refrigerant R134a, refrigerant R134a + 0.25% Al₂O₃ and refrigerant R134a + 0.40% Al₂O₃.

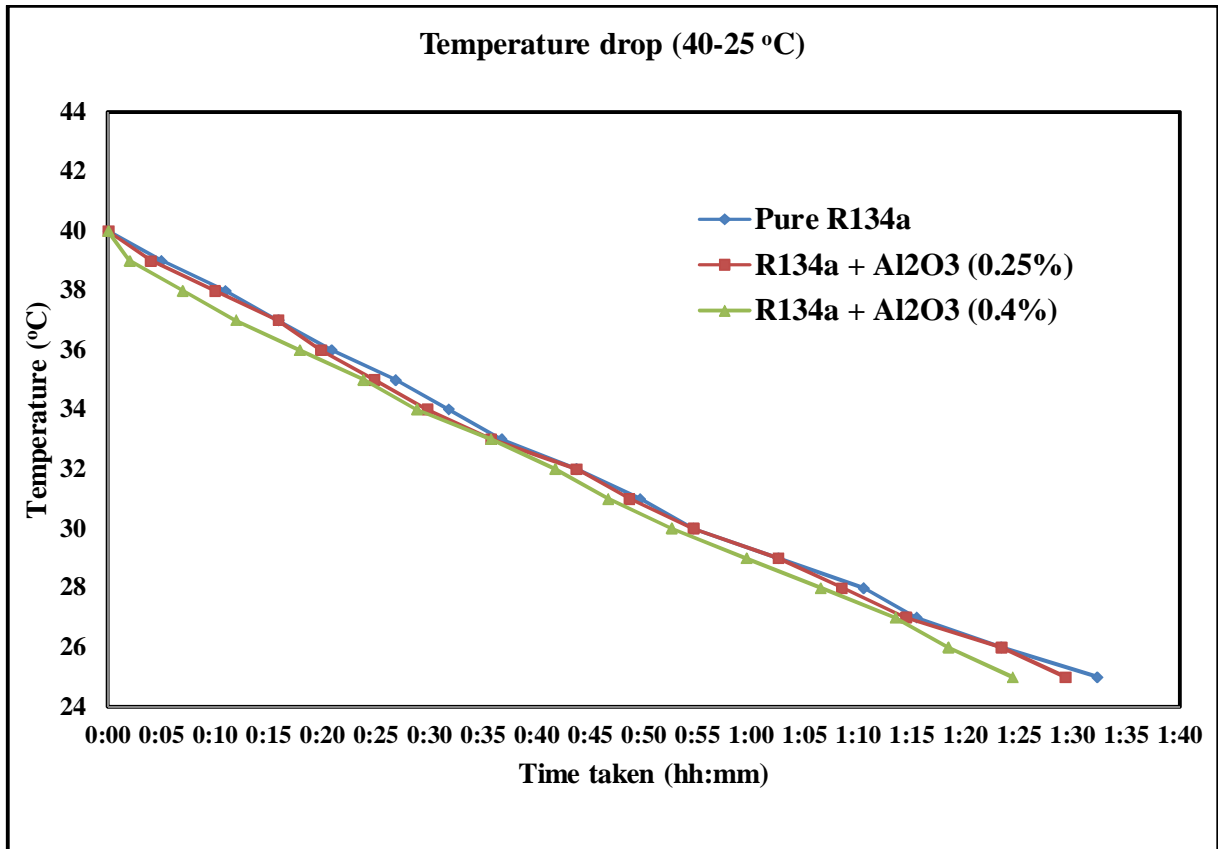


Fig.6.13: Temperature-time graph for refrigerant R134a and Al₂O₃ based nanorefrigerants at 11 LPH volume flow rate

Fig.6.13 represents the cooling load temperature - time analysis at 11 LPH volume flow rate for pure refrigerant R134a, refrigerant R134a + 0.25% Al₂O₃ and refrigerant R134a + 0.40% Al₂O₃ at ambient temperature 32°C ±1°C. In this study it is found that pure refrigerant R134a takes 1 hour 33 minutes for temperature drop from 40°C to 25°C, while nanorefrigerant R134a +0.25% Al₂O₃ takes 1 hour 30 minutes. While nanorefrigerant R134a +0.40% Al₂O₃ takes 1 hour 25 minutes for temperature drop from 40°C to 25°C. So, a decrease in time by 3.23% for refrigerant R134a +0.25% Al₂O₃ and by 8.6% for refrigerant R134a +0.40% Al₂O₃ for a temperature drop from 40°C to 25°C have been observed. This indicates heat transfer increases as concentration increases and takes less time to achieve a desired temperature.

6.7 Cooling load temperature - time analysis at 11 LPH volume flow rate for refrigerant R134a, SiO₂ and Al₂O₃ nanoparticles based nanorefrigerants

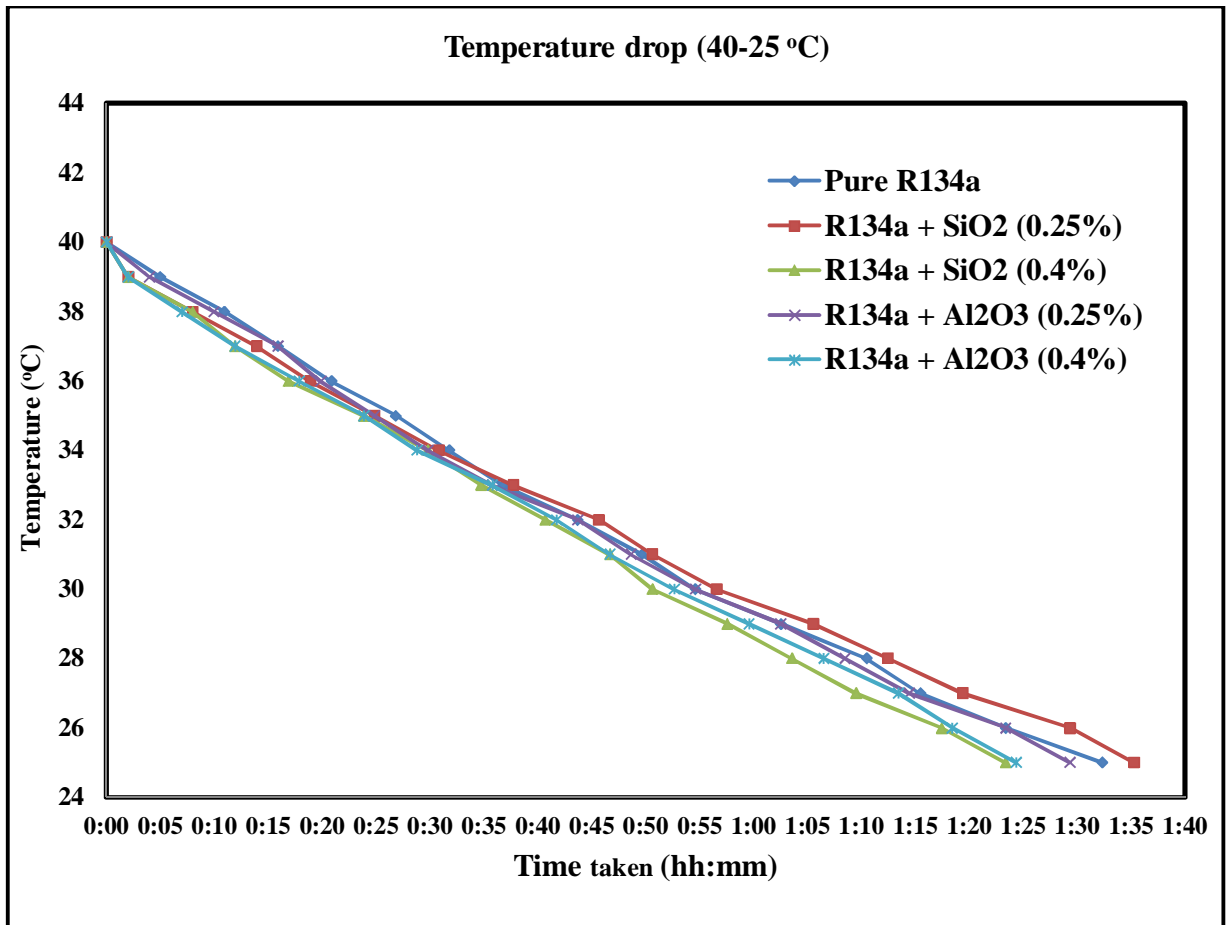


Fig.6.14: Temperature-time graph for nanorefrigerants at 11 LPH volume flow rate

Fig.6.14 represents temperature-time graph for a temperature drop from 40°C to 25°C at 11 LPH volume flow rate for refrigerant R134a, refrigerant R134a + 0.25% Al₂O₃, refrigerant R134a + 0.40% Al₂O₃, refrigerant R134a + 0.25% SiO₂ and refrigerant R134a + 0.40% SiO₂. It has been observed that as concentration increases the time taken to achieve desired temperature is reduced.

6.8 Power consumption for cooling load temperature - time analysis

Power input to the refrigeration system is an important parameter as COP of the system is dependent on it. Power consumed by the compressor to reduce temperature from 40°C to 25°C has been observed for pure refrigerant R134a, refrigerant R134a + 0.25% Al₂O₃, refrigerant R134a + 0.40% Al₂O₃, refrigerant R134a + 0.25% SiO₂ and refrigerant R134a + 0.40% SiO₂.

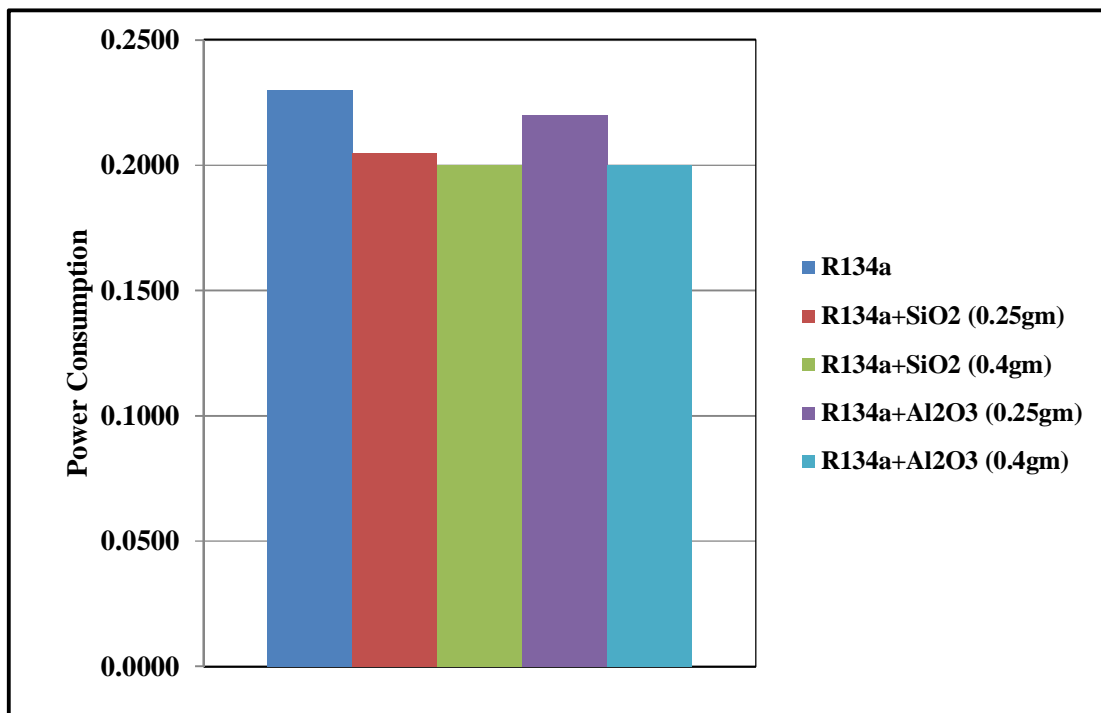


Fig.6.15: Power consumption by nanorefrigerants for temperature drop from 40°C to 25°C

In order to investigate the power consumption for cooling load temperature - time analysis following studies have been performed with pure refrigerant R134a, refrigerant R134a + 0.25% SiO₂, refrigerant R134a + 0.40% SiO₂, refrigerant R134a + 0.25% Al₂O₃ and refrigerant R134a + 0.40% Al₂O₃. Fig.6.15 shows power consumption for 40°C to 25°C temperature drop at 11 LPH volume flow rate. Ambient temperature is found to be around 31.5°C ±2°C. In this study it is found that pure R134a consumes 0.23 kWh for temperature reduction from 40°C to 25°C, while nanorefrigerant R134a + 0.25% SiO₂ consume 0.205kWh. Nanorefrigerant R134a +

0.40% SiO₂ consume 0.20 kWh and nanorefrigerant R134a + 0.25% Al₂O₃ and R134a + 0.40% Al₂O₃ consume 0.22 kWh and 0.20 kWh respectively. Figure also shows 10.87% & 13.04% reduction in power consumption for nanorefrigerant R134a + 0.25% SiO₂ and nanorefrigerant R134a + 0.40% SiO₂ as compared to refrigerant R134a. Reduction in power consumption for nanorefrigerant R134a + 0.25% Al₂O₃ and nanorefrigerant R134a + 0.40% Al₂O₃ is found to be 4.35% and 13.04% respectively as compared to refrigerant R134a. It has been observed that as concentration of Al₂O₃ & SiO₂ nanoparticles increases the power input to the refrigeration system decreases.

CONCLUSION AND FUTURE SCOPE

7.1 Conclusions

The present research work entitled “An Experimental Investigations into the Performance of Nanorefrigerants (R134a+Al₂O₃, R134a+SiO₂) Based Refrigeration System” was aimed at, to use nanoparticles in conjunction with R134a refrigerant. It has been decided to use nanoparticles Al₂O₃ and SiO₂ of size 60-70 nm each. Two concentrations of nanoparticles were taken to compare performance with pure refrigerant R134a.

- (i) The system was charged with nanorefrigerant R134a + Al₂O₃ and nanorefrigerant R134a + SiO₂ with 0.25 gm mass and 0.40 gm mass of nanoparticles
- (ii) All readings were taken at 11LPH volume flow rate and for two heat fluxes in evaporator at temperature 25–26 °C and 35–36 °C
- (iii) Temperature drop in condenser, temperature gain in evaporator, COP for the system and temperature-time chart were studied for both nanoparticles at both concentrations
- (iv) It was found that addition of aluminium oxide and silicon oxide nanoparticles to the refrigerant results in improvement in the thermo physical properties and heat transfer characteristics of the refrigeration system
- (v) It was observed that there is more temperature drop across the condenser for the nanorefrigerant (5.47% – 4.83%) compared to refrigerant R134a. Similarly, a gain of 6.89% and 8.08% was obtained for evaporator temperature. An improvement in COP was also observed during the investigations (1.17% – 8.40%). This was achieved under 25–26 °C evaporator temperature load

- (vi) Similar improvements were also observed when refrigeration system is operated at 35–36 °C evaporator temperature
- (vii) A reduction in the power consumption (10.87% & 13.04%) along with faster cooling (from 40°C – 25°C) is also achieved when nanorefrigerants are used
- (viii) The experimental studies indicated that the refrigeration system with nanorefrigerant works normal like any conventional refrigeration system
- (ix) Refrigerating effect was increased with the increase in concentration

7.2 Challenges & Future scope

The present research work was aimed at only two types of nanoparticles, two concentrations and single refrigerant. But there are number of other parameters available which can be varied and system performance can be studied.

- (i) Different concentrations of nanoparticles can be used
- (ii) There are number of refrigerants other than refrigerant R134a can be used to investigate the performance
- (iii) Systems can be made automatic using digital temperature and pressure gauges and other sensors
- (iv) System can be tried for different flow rates, at different evaporator loads, in different environment conditions, with Different amount of refrigerant mass
- (v) Nanoparticles can be used with in the evaporator water or in evaporator loading system
- (vi) System can be investigated in order to see the performance of air conditioning system along with vapour compression system
- (vii) System can be made to work with range of nanoparticles in lubricant oils in different concentrations

REFERENCES

- [1] Bi, S., Shi, L. and Zhang, L., 2007, 'Performance study of a domestic refrigerator using R134a/mineral oil/nano-TiO₂ as working fluid,' *ICR07-B2-346*.
- [2] Bi, S., Guo, K., Liu, Z. and Wu, J., 2011, 'Performance of a domestic refrigerator using TiO₂-R600a nano-refrigerant as working fluid,' *Energy Conversion and Management*, Vol. 52, pp.733–737.
- [3] Bozorgan, N., Kumar, K., Bozorgan, N., 2012, 'Numerical Study on Application of CuO-Water Nanofluid in Automotive Diesel Engine Radiator,' *Modern Mechanical Engineering*, Vol. 2, pp.130-136.
- [4] Choi, S.U.S., 1995, 'Enhancing thermal conductivity of fluids with nanoparticles,' *ASME FED 231*, Vol. 66, pp. 99–103.
- [5] Choi, S.U.S., Zhang Z. G., Yu, W., Lockwood, F.E. and Grulke, E.A., 2001, 'Anomalous thermal conductivity enhancement in nanotube suspensions,' *Applied. Physics Letters*, Vol. 79, pp. 2252.
- [6] Chopkar, M., Sudarshan, S., Das, P.K. and Manna, I., 2008, 'Effect of particle size on thermal conductivity of nanofluid,' *Metallurgical and Materials Transactions. ,* Vol.39A, pp.1535.
- [7] Clancy, E.V., 2012, 'Patent application title: Apparatus and method of using Nanofluids to improve energy efficiency of Vapor Compression Systems,' *Patent application number: 20120017614*.
- [8] Coumaressin, T., Palaniradja, K., 2014, 'Performance Analysis of a Refrigeration System Using Nano Fluid,' *International Journal of Advanced Mechanical Engineering*, Vol. 4, pp. 459-470.

- [9] Ding, G., 2007, 'Recent developments in simulation techniques for vapour-compression refrigeration systems,' *International Journal of Refrigeration*, Vol. 30, pp. 1119-1133.
- [10] Eastman, J.A., Choi, S.U.S., Li, S., Yu, W. and Thomson, L.J., 2001, 'Anomalously increased effective thermal conductivities of ethylene glycol based nanofluids containing copper nanoparticles,' *Applied Physics Letters*, Vol. 78, pp. 718.
- [11] Eiyad, A.N., 2008, 'Application of nanofluids for heat transfer enhancement of separated flows encountered in a backward facing step,' *International Journal of Heat and Fluid Flow*, Vol. 29, pp. 242–249.
- [12] Gupta, H.K., Agrawal, G.D., Mathur, J., 2012, 'An overview of Nanofluids: A new media towards green environment,' *International Journal of environmental science*, Vol. 3, No 1.
- [13] Hafez, E.A., Taher, S.H., Torki, A.H.M. and Hamad, S.S., 2011, 'Heat Transfer Analysis of Vapor Compression System Using Nano Cuo-R134a,' *International Conference on Advanced Materials Engineering. IPCSIT*, Vol. 15.
- [14] Jwo, C.S., Jeng, L.Y., Teng, T.P. and Chang, H., 2009, 'Effect of nano lubricant on the performance of Hydrocarbon refrigerant system,' *J. Vac. Science Technology*, Vol. 27, pp. 1473-1477.
- [15] Kumar, R.R., Sridhar, K., Narasimha, M., 2013, 'Heat transfer enhancement in domestic refrigerator using R600a/mineral oil/nano- Al_2O_3 as working fluid,' *International Journal of Computational Engineering*, Vol. 03, pp. 42-50.
- [16] Kumar, S.D. and Elansezhian, R., 2012, 'Experimental Study on Al_2O_3 -R134a Nano Refrigerant in Refrigeration System,' *International Journal of Modern Engineering Research*, Vol. 2, Issue. 5, pp. 3927-3929.

- [17] Lee, S., Choi, S.U.S., Li, S. and Eastman, J.A., 1999, 'Measuring thermal conductivity of fluids containing oxide nanoparticles,' *ASME J. Heat Transfer*, Vol. 121, pp. 280-89.
- [18] Loaiza, J.C.V., Pruzaesky, F.C., Parise, J.A.R., 2010, 'A Numerical Study on the Application of Nanofluids in Refrigeration Systems,' *International Refrigeration and Air Conditioning Conference at Purdue*, pp. 2495.
- [19] Loaiza, J.C.V., Pruzaesky, F.C. and Parise, J.A.R., 2010, 'Numerical Study on the Application of Nanofluids in Refrigeration Systems,' *International Refrigeration and Air Conditioning Conference*, pp. 1145.
- [20] Mahbubul, I.M., Saidur, R. and Amalina, M.A., 2012, 'Investigation of viscosity of R123-TiO₂ Nanorefrigerant,' *International Journal of Mechanical and Materials Engineering*, Vol. 7, pp. 146-151.
- [21] Mamut, E., 2006, 'Characterization of Heat and Mass Transfer Properties of Nanofluids,' *Rom. Journal Physics*, Vol. 51, pp. 5–12.
- [22] Masuda, H., Ebata, A., Teramae, K., Hishinuma, N., 1993, 'Alteration of thermal conductivity and viscosity of liquid by dispersing ultrafine particles (dispersion of c-Al₂O₃, SiO₂, and TiO₂ ultra-fine particles)', *Netsu Bussei.*, Vol. 4, pp.227.
- [23] Maxwell, J.C., 1873, 'A Treatise on Electricity and Magnetism,' *Oxford: Clarendon*.
- [24] Pang, C., Kang, Y.T., 2012, 'Stability and Thermal Conductivity Characteristics of Nanofluids (H₂O/CH₃OH+NaCl+Al₂O₃ Nanoparticles) for CO₂ Absorption Application,' *International Refrigeration and Air Conditioning Conference at Purdue*, pp. 2161.

- [25] Pantzali, M.N., Kanaris, A.G., Antoniadis, K.D., Mouzaa, A.A. and Paras, S.V., 2009, 'Effect of nanofluids in the performance of a miniature plate heat exchanger with modulated surface,' *International Journal of Heat and Fluid Flow*, Vol. 30, pp. 691-699.
- [26] Parise, J.A.R., Tiecher, R.F.P., 2012, 'A Simulation Model for the Application of Nanofluids as Condenser Coolants in Vapor Compression Heat Pumps,' *International Refrigeration and Air Conditioning Conference at Purdue*, pp. 2531.
- [27] Pawel, K.P., Jeffrey, A.E. and David, G.C., 2005, 'Nanofluids for thermal transport', *Materials Today*, pp. 36-44.
- [28] Peng, H., Ding, G., Haitao, H., 2011, 'Influences of refrigerant-based nanofluid composition and heating condition on the migration of nanoparticles during pool boiling. Part I: Experimental measurement,' *International journal of refrigeration*, Vol. 34, pp. 1823-1832.
- [29] Subramani, N., Prakash, M.J., 2011, 'Experimental studies on a vapour compression system using nanorefrigerants,' *International Journal of Engineering, Science and Technology*, Vol. 3, pp. 95-102.
- [30] Wang, K.J, Ding, G.L., Jiang, W.T., 2006, 'Nano-scale thermal transporting and its use in engineering,' *4th Symposium on Refrigeration and Air condition*, Southeast University Press, Nanjing, China, pp. 66-75.
- [31] Wang, X., Xu, X. and Choi, S.U.S., 1999, 'Thermal conductivity of nanoparticle- fluid mixture', *J. Thermal Physics Heat Transfer*, Vol. 13, pp. 474.
- [32] Xie, H., Wang, J., Xi, T., Liu, Y., 2002a, 'Thermal conductivity of suspensions containing nanosized SiC particles', *International Journal Thermo physics*, Vol. 23, pp. 571.

APPENDIX

S. No.	Description of item	Qty	Specification	Cost (Rs.)
1	Al ₂ O ₃ nanoparticle	20gm	60-70nm	2100
2	SiO ₂ nanoparticle	20gm	60-70nm	800
3	Copper pipe	9 meter	¼ Inch	750
4	Soldering material			100
5	Voltmeter	1		100
6	Compressor	1	165 Liter compressor	2500
7	Condenser	1	Finned static condenser	300
8	Filter	1		20
9	Rotameter	1	4-40LPH	4080
10	Expansion valve (Manual)	1	Hand operated	500
11	Evaporator	7.5 meter	¼ inch	650
12	Heater	1	2000 watt	300
13	Rubber pipe	1	20 feet	100
14	Digital temperature controller	1		1000
15	Refrigerant charging line	1		200

16	Pressure gauge	1	Two low, Two high pressure	500
17	Energy meter	2		Lab
18	Main switch	1		500
19	Refrigerant	1000gm	R134a	600
20	Wiring			500
21	Insulation	5 meter	For ¼ inch pipe	100
22	Valve	4	¼ inch	1100
23	Acetylene gas cylinder	2		300
24	Flare nut	20	¼ inch	300
25	T and clamps	15	¼ inch	2000
26	Nut and bolt	20		200
27	Stainless steel drum	1		400
28	Ampere meter	1		100
29	Miscellaneous			1000
30	Total			21100

Table A1: Cost estimation